AERODYNAMIC ANALYSIS OF LONG-SPAN BRIDGE CROSS-SECTIONS USING RANDOM VORTEX METHOD

A THESIS SUBMITTED TO
THE GRADUATE SCHOOL OF NATURAL AND APPLIED SCIENCE
OF
MIDDLE EAST TECHNICAL UNIVERSITY

BY

HALİL KAYA

IN PARTIAL FULFILLMENT OF THE REQUIREMENTS
FOR
THE DEGREE OF MASTER OF SCIENCE
IN
AEROSPACE ENGINEERING

SEPTEMBER 2012

Approval of the thesis:

AERODYNAMIC ANALYSIS OF LONG-SPAN BRIDGE CROSS-SECTIONS USING RANDOM VORTEX METHOD

submitted by **Halil KAYA** in partial fulfillment of the requirements for the degree of **Master of Science in Aerospace Engineering Department, Middle East Technical University** by,

Prof. Dr. Canan Özgen _____
Dean, Graduate School of **Natural and Applied Sciences**

Prof. Dr. Ozan Tekinalp _____
Head of Department, **Aerospace Engineering**

Assoc. Prof. Dr. Oğuz Uzol _____
Supervisor, **Aerospace Engineering Dept., METU**

Examining Committee Members

Prof. Dr. Serkan Özgen _____
Aerospace Engineering Dept., METU

Assoc. Prof. Dr. Oğuz Uzol _____
Aerospace Engineering Dept., METU

Prof. Dr. İsmail Hakkı Tuncer _____
Aerospace Engineering Dept., METU

Prof. Dr. Yusuf Özyörük _____
Aerospace Engineering Dept., METU

Asst. Prof. Dr. Özgür Kurç _____
Civil Engineering Dept., METU

Date: 27.09.2012

I hereby declare that all information in this document has been obtained and presented in accordance with academic rules and ethical conduct. I also declare that, as required by these rules and conduct, I have fully cited and referenced all material and results that are not original to this work.

Name, Last Name: Halil KAYA

Signature:

ABSTRACT

AERODYNAMIC ANALYSIS OF LONG-SPAN BRIDGE CROSS-SECTIONS USING RANDOM VORTEX METHOD

Kaya, Halil

M.S., Department of Aerospace Engineering

Supervisor: Assoc. Prof. Dr. Oğuz Uzol

September 2012, 75 pages

In this thesis, two dimensional, incompressible, viscous flow past bluff bodies and a bridge section, in which strong vortex shedding and unsteady attribute of flow are generally found, is simulated by means of random vortex method.

The algorithm and method are described in detail. The validation and applicability of the developed numerical implementation to general wind engineering problems is illustrated by solving a number of classical problems, such as flow past circular and square cylinders. An application of the numerical implementation in the area of computational wind engineering is performed by analyzing a bridge deck section. Moreover, all results are compared with experimental and numerical studies in literature.

Keywords: Computational Wind Engineering, Random Vortex Method, Bluff Body Aerodynamics

ÖZ

UZUN AÇIKLIKLI KÖPRÜ KESİTLERİNİN RASTGELE GİRDAP METODU İLE AERODİNAMİK ANALİZİ

Kaya, Halil
Yüksek Lisans, Havacılık ve Uzay Mühendisliği Bölümü
Tez Yöneticisi: Assoc. Prof. Dr. Oğuz Uzol
Eylül 2012, 75 sayfa

Bu tezde, güçlü girdap salınımlarının ve durağan olmayan davranışların sıkça görüldüğü küt cisimler ve bir köprü kesitinden geçen iki boyutlu, sıkıştırılamayan, sürtünmeli akımların simülasyonu gerçekleştirilmiştir.

Kullanılan algoritma ve metot detayları ile anlatılmıştır. Geliştirilen nümerik uygulamanın genel rüzgar mühendisliği uygulamalarında geçerliliği ve uygulanabilirliği, dairesel ve kare kesitli silindir üzerinden geçen akım çözülerek gösterilmiştir. Elde edilen değerlerin mevcut deneysel ve nümerik çalışmalarla kıyaslamaları da yapılmıştır.

Anahtar Kelimeler: Hesaplamalı Rüzgar Mühendisliği, Rastgele Girdap Metodu, Küt Cisim Aerodinamiği

Dedicated to my family

ACKNOWLEDGEMENTS

This dissertation would not have been possible without the guidance and the help of several individuals who in one way or another contributed and extended their valuable assistance in the preparation and completion of this study.

First and foremost, I would like to thank my supervisor Assoc. Prof. Dr. Oğuz Uzol for his guidance support, encouragement, indulge and patience throughout the study.

I also would like to thank;

Erhan Tarhan, Gürkan Çetin and Ethem Hakan Orhan for their understanding and tolerance.

Ali Ruhşen Çete, Erhan Tarhan and departed Hacı İbrahim Keser, for their technical supports they gave.

Hande Akalan, Emre Dede and Hakkı Özgür Derman for editing the dissertation.

My colleagues and my friends, for their endless moral support.

Last but not the least, my brother Anıl Kaya, for his moral support and encouragements.

TABLE OF CONTENTS

LIST OF TABLES

TABLES

LIST OF FIGURES

FIGURES

LIST OF SYMBOLS

LATIN SYMBOLS

A	Area
B	Width of bridge deck section
c	Chord length of airfoil
cd	Drag coefficient
cl	Lift coefficient
CWE	Computational Wind Engineering
D	Diameter of circle or height of bridge deck section
DNS	Direct Numerical Simulation
e	Exponential
f	Shedding frequency
h	Grid space
ISA	International Standard Atmosphere
K	Cauchy velocity kernel
L	Characteristic length
LES	Large Eddy Simulation
m	meter
M	Number of line segment elements
N	Number of particles
n	Normal direction
U	Velocity
p	Pressure
r	Radial component of polar coordinates

Re Reynolds number

r.m.s Root mean square

RVM Random Vortex Method

s Panel length

St Strouhal number

t Time

V Velocity

x,y Components of cartesian coordinates

GREEK SYMBOLS

α Side angle

γ Surface vorticity

Γ Strength of vorticity

ρ Density

ν Kinematic viscosity

ω Vorticity

ψ Stream function

CHAPTER 1

INTRODUCTION

Among all the natural events on the buildings and structures, wind is possibly the most damaging one. In relation to this, the effect of the flow on the structures has been an important research topic over the years. Wind engineers have always worked to predict the flow behavior and the effect of it on the structures, by using wind tunnels. With the help of advances in computer technology, by using mathematical models of the fluid flow, engineers have begun to develop numerical techniques to simulate fluid motion. Therefore, an individual discipline has appeared in wind engineering, such as Computational Wind Engineering (CWE).

Bluff body aerodynamics, especially building aerodynamics is an important research topic for wind engineers. During the design process of the buildings, to be able to construct buildings which are safer and less vulnerable to wind effects, engineers and architects have been both considering the influence of wind for the last few years. So accurate prediction of the flow behavior and the effect of it on the buildings is important. In this framework, wind engineers focus on simulation of the flow around bluff bodies, such as square, triangle, and circular cylinder, considering their simplicity and similarity to the building shapes.

Computational methods allow the study of fluid-structure interaction problem in detail and faster than experiments, costing less money and lowering risk factors. Moreover, it provides, in addition to pressures and wind loads, which wind tunnel

test can only predict, the flow field with velocity, temperature and vortex structures.

In bluff body aerodynamics, the interest in vortex methods boost notably. This interest is because of good results obtained for bluff bodies (at least for 2D cases) and it offers an alternative method to other numerical methods (e.g. Finite Element and Finite Volume Methods). They enjoy the simplicity of the vorticity form of the incompressible Navier-Stokes equations. In vortex methods, the vorticity field is discretized into the particles, and they are followed in a Lagrangian manner. So it provides some advantages as listed below;

- Vorticity is discretized only where its value is different from zero.
- Vortex methods are self-adaptive methods. Particles are always created where they are required and move to the interested area.
- Boundary condition at infinity is supplied automatically.
- Comparisons with Eulerian finite difference schemes has shown that vortex methods can be faster by up to an order of magnitude, even when the volume is completely filled with vorticity [1].

1.1 Literature Review

1.1.1 Early Researches

Many researchers have been interested in the structure of vortex street behind the bluff bodies since the early experiments of Strouhal [2] about `Aeolian tones` and Theodore von Karman's paper [3]. Historically, the study of Rosenhead [4] on the Kelvin-Helmholtz instability of vortex sheets is the first real dynamical vortex simulation which is done in two dimensions with 12 singular point vortices. Birkhoff & Fisher [5] repeated the same calculations with finer discretization.

Abernathy & Kronauer [6] used Rosenhead`s model to study on the stability of a parallel pair of infinite vortex sheets. Chorin & Bernard [7] and Kuwahara & Takami [8] made use of this method with regularized vortex cores, as a result they obtained smoother roll-up of the vortex sheet. For the first time, Hald [9] and Hald & Del Prete [10] proved the existence of a solution without viscosity, which requires the maintaining of the overlap between vortex core radius [11].

1.1.2 Random Walk Method

The Lagrangian nature of vortex methods encounters difficulties in simulating viscous effects. To deal with this problem, Chorin [12] suggested to use random walk method, which is a statistical approach based on the Brownian motion of fluid particles. This method suggested by Chorin is called Random Vortex Method (RVM). The results obtained by using this method have statistical noise. This method also has a low rate of convergence [13]. The method is, however, very easy to implement to simple geometries and also fully Langrangian approach for diffusion. Chorin [14] used this method to study boundary layer instability. Independently of Chorin, Porthouse & Lewis [15] developed a random walk technique to study boundary layer flows and to simulate the wake behind cylinder. So they pointed out the usefulness of vortex methods.

After Chorin and Porthouse & Lewis, random walk method is used in many researches to simulate diffusion. Chorin used his method for simulating fluid flow over cylinders [12], [16] and flat plates [14], [16], [17]. McCracken & Peskin [18] simulated using RVM the blood flow thorough heart valves. Ghoniem*et.al.* [19] modeled turbulent flow by using random walk method in a combustion tunnel. Moreover, he calculated the velocity field using Biot-Savat rule. The results of this simulation were in a good agreement with experimental one. Cheer [20], [21] simulated fluid flows over a cylinder and an airfoil for different

Reynolds number. His results are also in a good agreement with experimental results, even though fairly coarse computations. Sethian [22] modeled turbulent combustion inside a rectangular chamber again by using random walk method. The convergence of the method in 2D is studied by Mortazavi [23]. Gagnon [24] implemented this method to simulate the fluid flow over a single a double symmetrical backward-facing step. Kim and Flynn [25] studied the fluid flow over multiple bodies with the random walk method. They focused in flow patterns rather than quantitative measures. Wang [26] investigated dynamic stall of airfoils. Lin *et. al.* [27] is simulated with RVM pitching airfoil. Taylor & Vezza [28] used RVM to simulate the flow over rectangular cylinders and square. Ramachandran [29] studied flow over a circular cylinder using high-resolution RVM.

1.1.3 Remeshed Particle Methods

"The deterioration of the spatial accuracy of the vortex particle method is brought about by the separation of the individual vortices during their notion, causing a non-smooth representation of the vorticity field.
The primary methods to solve this problem are: recalculation of the quadrature weights at each time step [30], [31], [32], regridding/rezoning [33] (is this to new particles?), and global regridding to regularly- spaced particles" [34].

The necessity of remeshing is shown by Mansfield [35] in flows with high strain. Cottet [36] and others [37] implemented remeshing using a remapped grid with spatially-varying cell sizes. This method, which is a multi-resolution method, allows high resolution near wall and shedding and coarser resolution in far-field.

"A detailed description of the remeshing of elliptical particles to regular axisymmetric particles is done in [38]. Chatelain & Leonard [39] present a

method for particle redistribution to a face-centered cubic lattice, and show that it compares favorably with redistribution using M4' and "witch-hat" (M2) filters. Eldredge [40] remeshes every few steps using the M4' kernel.

Clearly, particle methods with remeshing are accurate and fast, but they are less useful to define sharp discontinuities." [34].

1.1.4 Application of Vortex Methods to the Structures

The vortex method has been used widely in computational wind engineering, to predict the flow around buildings and deck shapes.

In the paper [41], the RVM is used to study the flow of wind around common building shapes. Moreover, the results were compared with experimental data. Bui & Oppenheim [42] performed random vortex method to simulate the turbulent flow of air over a scale model building in wind tunnel. Turkiyyah, Reed & Yang [43] used the random vortex method for wind engineering simulations. They presented two dimensional flow simulations of atmospheric boundary layer wind flow around a bluff body under open terrain conditions. Bazeos & Beskos [44] presented a numerical methodology for determination of wind pressures on rigid civil engineering structures under two dimensional conditions. They numerically simulated by combining the direct boundary element method with the discrete vortex method. So, they concluded that their proposed methodology enables one to determine wind loads on those structures simply, rapid and with satisfactory accuracy. Moreover, Bienkiewicz & Kutz [45] used the vortex method to simulate flow around bluff body wind engineering applications. Preidikman & Mook [46] analyzed flutter suppression on their passive control mechanism using vortex methods.

The vortex method was also used to simulate deck shapes. Walther & Larsen [47] analyzed five different deck shapes, by using their vortex method based code DVMFLOW. They got fairly good results which were in good agreement with wind tunnel results. Taylor & Vezza [48], [49] undertook studies on sharp edged bodies using vortex methods. They also performed their numerical implementation to study bridge aerodynamics including flutter analyses. Morgenthal [50] analyzed various shapes generally structures (like Glasgow Wing Tower, The Millau Viaduct, The Neath Viaduct, Storebælt Bridge).

1.2 Objectives

The objective of this thesis is to develop a useful, reliable numerical tool which can simulate the flow field around bluff bodies in the framework of CWE, by using vortex methods and to analyze some bridge section with the developed code.

1.3 Thesis Organization

In CHAPTER 2, underlying governing equations, algorithm and numerical methodology of the present numerical implementation is explained in detail. In CHAPTER 3, validation and applicability of the random vortex method based numerical code is illustrated by solving general fluid dynamics problems, such as flow past a circular, a square cylinder and NACA 0012 airfoil. In CHAPTER 4, the developed random vortex method code is performed to analyze a general wind engineering problem which is flow around a bridge cross section. Moreover the results obtained with present numerical implementation are compared with experimental data. Finally, in CHAPTER 5 the discussion of the developed code

is made for applicability for wind engineering problems and future works are mentioned.

CHAPTER 2

NUMERICAL METHODOLOGY

2.1 Governing Equations

Consider a fluid, which has constant density and viscosity. Moreover, it is homogenous and temperature variation has no impact on it. The flow of such a fluid may be described in terms of velocity **u**(**x**,t) and pressure **p**(**x**,t) of the flow by the conservation of momentum as;

$$\frac{\partial \mathbf{u}}{\partial t} + \mathbf{u} \cdot \nabla \mathbf{u} = -\frac{1}{\rho} \nabla p + \nu \nabla^2 \mathbf{u} \tag{2.1}$$

Where $\rho$is denoted the density of the fluid and $\nu$is the kinematic viscosity of the fluid. The continuity equation is written as;

$$\nabla \cdot \mathbf{u} = 0 \tag{2.2}$$

In vortex methods, these equations are used in velocity-vorticity formulation. To convert equations, it should be taken the curl of velocity. So the vorticity field (ω) is related to the velocity field as;

$$\boldsymbol{\omega} = \nabla \times \mathbf{u} \tag{2.3}$$

If the curl operator is applied to equation (2.1), the following expression is obtained;

$$\underbrace{\frac{D\boldsymbol{\omega}}{Dt}}_{\text{Convection}} = \underbrace{\boldsymbol{\omega} \cdot \nabla \mathbf{u}}_{\text{Streching}} + \underbrace{\nu \nabla^2 \boldsymbol{\omega}}_{\text{Diffusion}} \tag{2.4}$$

Where the material derivative is given as;

$$\frac{D}{Dt} = \frac{\partial(\ )}{\partial t} + \mathbf{u} \cdot \nabla(\quad) \tag{2.5}$$

When two dimensional flow is considered, $\boldsymbol{\omega}$ is normal to the plane of the flow, hence stretching term is zero.

In the context of random vortex methods proposed by Chorin [12], the equation is solved in two steps. Firstly, convection equation was solved which is;

$$\frac{D\boldsymbol{\omega}}{Dt} = 0 \tag{2.6}$$

Secondly, diffusion equation was solved which is;

$$\frac{\partial \boldsymbol{\omega}}{\partial t} = \nu \nabla^2 \boldsymbol{\omega} \tag{2.7}$$

This method is known as viscous/operator splitting technique. Thanks to this method, one can solve the equation (2.4) in a Lagrangian manner.

2.2 Determination of Velocity Field

To be able to develop the flow, the velocity field should be determined. If the velocity field is associated with a stream function $\boldsymbol{\psi}(\mathbf{x})$, the following equation is obtained;

$$\mathbf{u} = \nabla \times \boldsymbol{\psi} \tag{2.8}$$

Using the continuity equation (2.2) and the definition of vorticity (2.3), one can derive a Poisson equation, which is given as;

$$\nabla^2 \psi = -\omega \tag{2.9}$$

A general method to solve the Poisson equation to get the velocity field from the vorticity field is using Green's functions. So the velocity field can be determined using Green's function formulation for the solution of Poisson equation as;

$$\mathbf{u} = \mathbf{K} * \boldsymbol{\omega} = -\frac{1}{2\pi} \int \mathbf{K}(\mathbf{x} - \mathbf{y}) \times \boldsymbol{\omega}\, d\mathbf{y} + \mathbf{U}_{0(\mathbf{x},t)} \tag{2.10}$$

Where $\mathbf{U}_{0(\mathbf{x},t)}$ is the solution of the homogeneous Poisson equation and where

$$\mathbf{K}(\mathbf{x} - \mathbf{y}) = (\mathbf{x} - \mathbf{y})/|\mathbf{x} - \mathbf{y}|^2 \tag{2.11}$$

is the Cauchy velocity kernel. The equation (2.10) is called Biot-Savart law.

2.3 Discretization of Surface

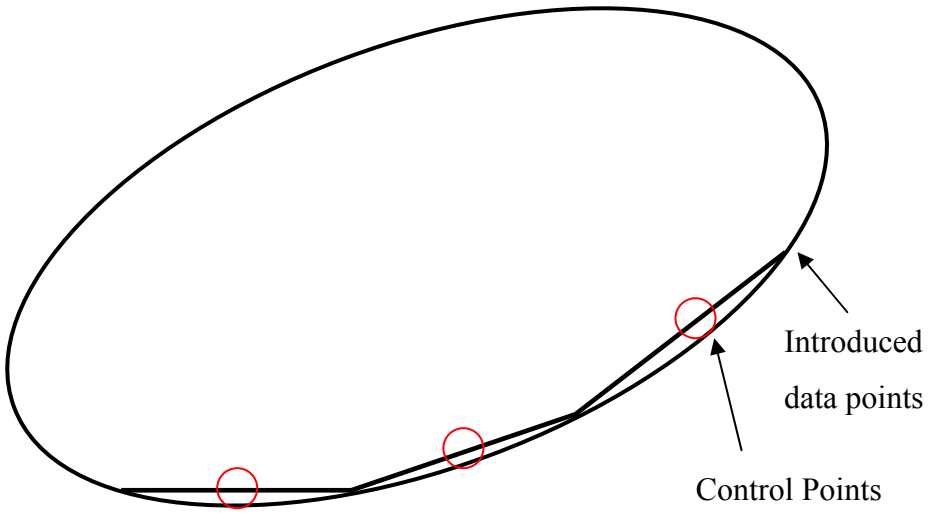

Figure 2-1 Discrete surface model

The solid surface is discretized by introducing M+1 data coordinates on its boundary (Figure 2-1). M straight line elements having length Δs_i are obtained by joining successive data points. The control points of straight line elements are defined at middle of each panel i at which boundary condition is imposed.

2.4 Boundary Condition at Surface

For a viscous flow, both normal and tangential components of the velocity on the wall should be equal to zero. Here, to ensure no-slip boundary condition on the surface, Dirichlet type boundary condition is applied. It is enough to satisfy that the tangential velocity on the wall is equal to the velocity of the wall, because this is equivalent to using the no-penetration boundary condition, and proof is supplied by Lewis [51].

The boundary condition is ensured on the wall by following these steps:

- The induced velocity on the surface is calculated by using Biot-Savart law, so the slip velocity on the wall is obtained.
- Then the surface vorticity is solved by ensuring the no-slip boundary condition ($U_{body}=U_{@surface}$).

2.5 Convection

The convection equation stands together with Euler equation in vorticity formulation (2.6). It means that "In an inviscid fluid a vortex tube moves with the fluid and its strength remains constant." Helmholtz first theorem. So that makes the equations well-suited to Lagrangian approach.

The integral in equation (2.10) may be discretized to get an approximation of the velocity field. For the present numerical scheme, the vorticity field is discretized by N point vortices, at $\mathbf{x}$, with circulation Γ_j. Therefore, the convection is implemented as;

$$\frac{\partial \mathbf{x}_p}{\partial t} = \mathbf{U}_\infty - \frac{1}{2\pi} \sum_{i=1, i\neq p}^{N_i} \frac{\boldsymbol{\Gamma}_i \times (\mathbf{x}_p - \mathbf{x}_i)}{\left|\mathbf{x}_p - \mathbf{x}_i\right|^2} \tag{2.12}$$

Where $\boldsymbol{\Gamma}_p = \Gamma_p \mathbf{k}$.

Hence, according to the equation (2.12) advection is implemented. Moreover, as a time integration scheme, first order Runga-Kutta method is used.

2.6 Vortex Release Algorithm

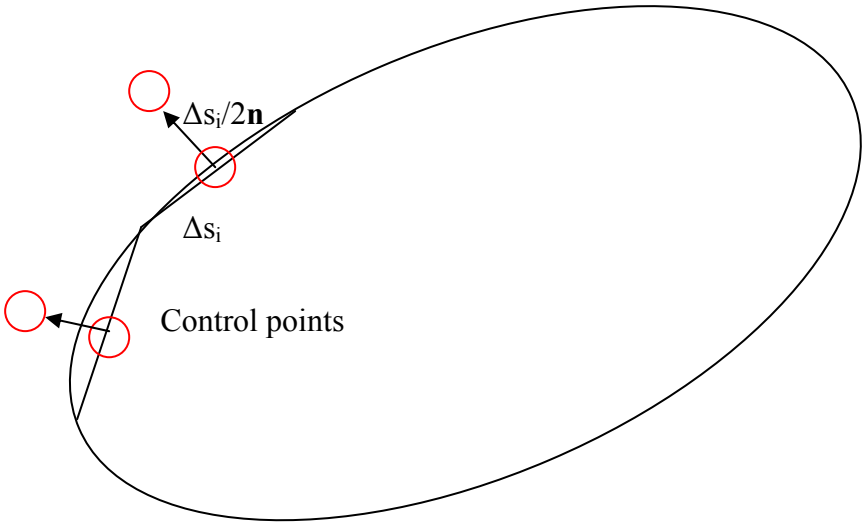

Figure 2-2 Vortex release method

In vortex methods, vorticity is created at wall. While time-dependent simulation vorticity is created on the surface of the solid body as a vortex-sheet with vorticity value $\gamma_i \Delta s_i$ which is computed to ensure no-slip condition. Then, they are released to the flow field as vortex particles, from mid-points of the panels in the normal direction with a distance of half a panel length (Figure 2-2).

2.7 Remeshing Method

"Particle methods are often defined as grid-free methods making them an attractive alternative to mesh based methods for flows past complex and deforming boundaries. However the adaptivity provided by the Lagrangian description can introduce errors and particle methods have to be conjoined with a grid to provide consistent, efficient and accurate simulations. The grid does not

detract from the adaptive character of the method and serves as a tool to restore regularity in the particle locations via *Remeshing* while it simultaneously enables systematic *Multiresolution* particle simulations [52], allows fast velocity evaluations [53] and facilities Hybrid particle-Mesh methods capable of handling different numerical methods and different equations in various parts of the domain [54]." [55].

Thus, to maintain accuracy by regulating particles and to be able to perform faster analyses a remeshing method is performed at every step. Moreover, significantly time savings is obtained by generating an influence matrix of grid to grid interaction at the beginning of the simulation.

Remeshing is employed as follows:

- Distribute each particles strength of vorticity to corners of the cell which is occupied by the particle, by using bilinear weighting scheme (Figure 2-3);

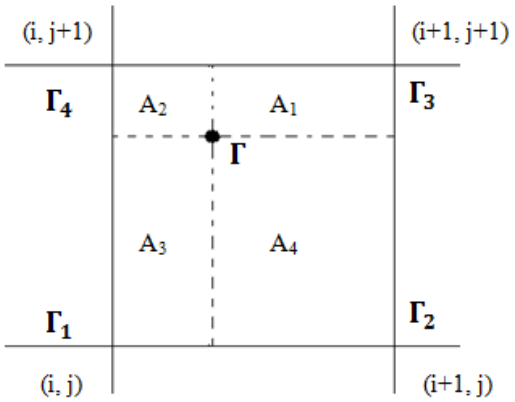

$$\Gamma_i = \Gamma \cdot A_i / \sum_{k=1}^{4} A_k$$

Figure 2-3 Vorticity distribution to the cell corners

- After all distribution process is completed, the total circulation of a mesh point is equal to total contribution of all vortices.
- Then velocity at each mesh point is calculated according to Biot-Savart law.
- Finally, the velocities at mesh points are redistributed to discrete vortex points according to bilinear weighting scheme (Figure 2-4).

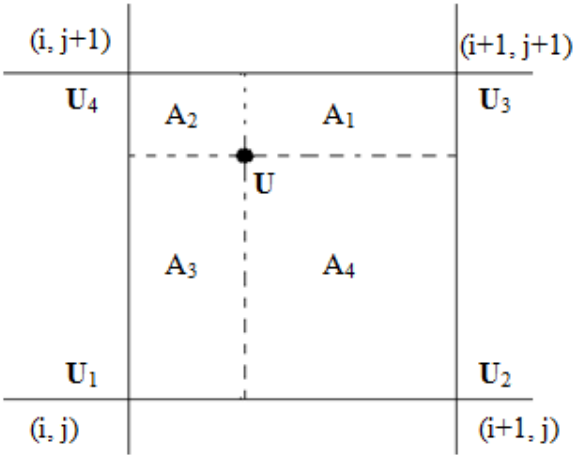

$$\mathbf{U}_i = \mathbf{U} \cdot \mathbf{A}_i / \sum_{k=1}^{4} \mathbf{A}_k$$

Figure 2-4 Redistribution of velocity to the particles

2.7.1 Results

In this subsection, the effect of particle remeshing implemented herein is investigated. As a reference case, flow around a circular cylinder at Reynolds number 1000 is solved. Moreover, the grid used is a fixed square grid with the particle grid spacing, $\Delta h = 0.1$ D.

Since the important parameter for the flow past bridge analysis is vortex shedding frequency, the results of the lift oscillation, from which vortex shedding frequency could be derived, obtained with/without remeshing is compared.

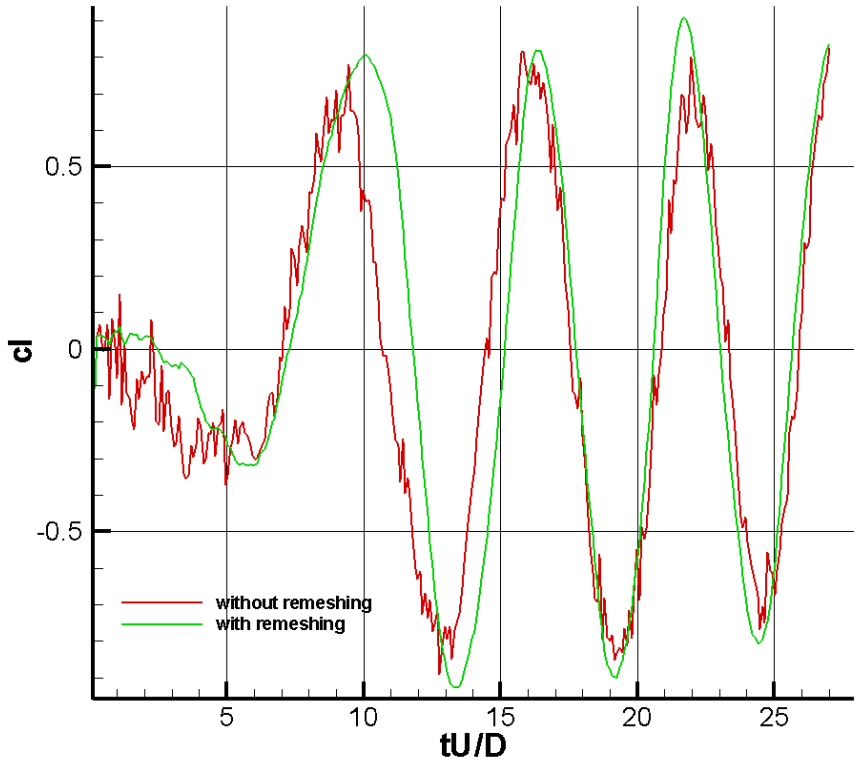

Figure 2-5 Time history of lift coefficients of flow around a circular cylinder analysis at Re = 1000, with/without remeshing

Table 2-1 Comparison of Strouhal number obtained from uniform flow past a circular cylinder analysis at Re = 1000 for time 18-25 s, with/without remeshing

Re	Without remeshing	With remeshing	Difference(%)
1000	0.167	0.174	4.1

According to the graph (Figure 2-5), it is seen that the result obtained without remeshing method is noisy. But the Strouhal numbers, which are important to get accurately for flow past bridge analyses, of analyses are close to each other (Table 2-1). Moreover, the result with remeshing is closer to the experimental result of ≈0.2 (Figure 3-11). Furthermore, the required time to run the simulation without grid is 5562.56 seconds, however the required time to run the simulation with grid is only 427. 34 seconds.

2.8 Diffusion

According to operator/viscous splitting technique, convection and diffusion are treated independent of each other. Convection method is already described in section 2.5.

To solve the diffusion part of the equation (2.4), in this thesis, random walk method is employed.

2.8.1 Random Walk Method

The governing equation for diffusion can be written as in polar coordinates;

$$\frac{\partial \boldsymbol{\omega}}{\partial t} = \nu \left\{ \frac{\partial^2 \boldsymbol{\omega}}{\partial r^2} \pm \frac{1}{r} \frac{\partial \boldsymbol{\omega}}{\partial r} \right\} \tag{2.13}$$

By using Green's function to solve the equation (2.13), it can be obtained the solution for the subsequent vorticity distribution, Batchelor [57].

$$\boldsymbol{\omega}(r,t) = \frac{\boldsymbol{\Gamma}}{4\pi\nu t} e^{\left(-\frac{r^2}{4\nu t}\right)} \tag{2.14}$$

The random walk method employed in the present study is depended on a numerical solution of the equation by discrete vortex particles, as developed by Porthouse & Lewis [15]. This method is actually a probabilistic interpretation of Green's function integral solution.

According to this method, all vortex particles are independently subjected to a random Gaussian displacement with zero mean and variance $2\nu\Delta t$. The equation (2.14) is simulated in the present numerical implementation as;

$$\mathbf{x}_{p,diffused} = \mathbf{x}_p + \mathbf{r}_p \tag{2.15}$$

Where $\mathbf{r}_p$is a vector that satisfies the equation (2.13) in a statistical manner. Therefore, the method is stochastic and the solution is noisy. The method is shown to have a convergence rate $O(\sqrt{\nu/N})$ by Roberts [56]. Hence, this is a slow rate of convergence. However, the method is used to solve a variety of problems as discussed in the section 1.1.2.

2.9 Replacement of Particles Crossing Body Surface and Vortex Deletion

If a vortex particle enters inside the body, this particle should be annihilated, absorbed from the surface panels or moved back on the body surface. In the present study, it is preferred moving back the particle, if it enters inside the body surface. This method was found to produce more stable results than deletion in certain cases [50].

A particle which enters inside the solid region is moved back perpendicular to the nearest panel with the normal distance of the particle to their nearest panel.

If a vortex particle travels beyond a certain cut-off distance, its effect on the vortex shedding becomes negligible. So, the vorticity domain is limited with the fifteen times of the length of the body, and the particle that travels beyond that limitation is deleted.

2.10 Pressure Calculation

The surface pressure is calculated from vorticity flux on the surface. The momentum equation is given as;

$$\frac{\partial \mathbf{u}}{\partial t} + \mathbf{u} \cdot \nabla \mathbf{u} = -\frac{1}{\rho} \nabla p + \nu \nabla^2 \mathbf{u} \tag{2.16}$$

After taking the dot product of the equation with the tangential vector of the body surface;

$$\frac{DU_s}{Dt} = -\frac{1}{\rho} \frac{\partial p}{\partial s} - \nu \frac{\partial \omega}{\partial n} \tag{2.17}$$

Where *s* and *n* mean respectively, the tangential and normal direction of the surface panels.

If the surface is assumed to have constant velocity, the left hand side is equal to zero, and the equation reduces to;

$$\frac{1}{\rho}\frac{\partial p}{\partial s} = -\nu\,\frac{\partial \omega}{\partial n} \tag{2.18}$$

The right hand side term represents the vorticity creation at the surface. Thus, vortex sheet with strength γ is released at a given time on the wall. So a relation can be established as;

$$\nu\,\frac{\partial \omega}{\partial n} = \frac{\partial \gamma}{\partial t} \tag{2.19}$$

Then combining the equations (2.18) and (2.19), the following equation is obtained;

$$\frac{\partial p}{\partial s} = -\rho\,\frac{\partial \gamma}{\partial t} \tag{2.20}$$

This equation can be discretized for the pressure gradient on the surface as;

$$\Delta p_i = -\rho\,\frac{\gamma_i \Delta s_i}{\Delta t} \tag{2.21}$$

Then pressure value at a panel on the surface is calculated as;

$$p_i = p_1 - \frac{\rho}{\Delta t}\sum_{j=1}^{i} \gamma_j \Delta s_j \tag{2.22}$$

Where $p_1$is a datum value (which is initially set as zero), from where the integration of the equation (2.22) begins for numerical convenience. Then the stagnation point is searched around leading edge, finally all pressure values are

increased an amount of $\frac{1}{2}\rho|\mathbf{U}_\infty|^2 - p_h$, where p_h is highest pressure around profile.

2.11 Computational Scheme

Having mentioned the theory and numerical implementation of the random vortex method, the computational scheme of the present code is illustrated below:

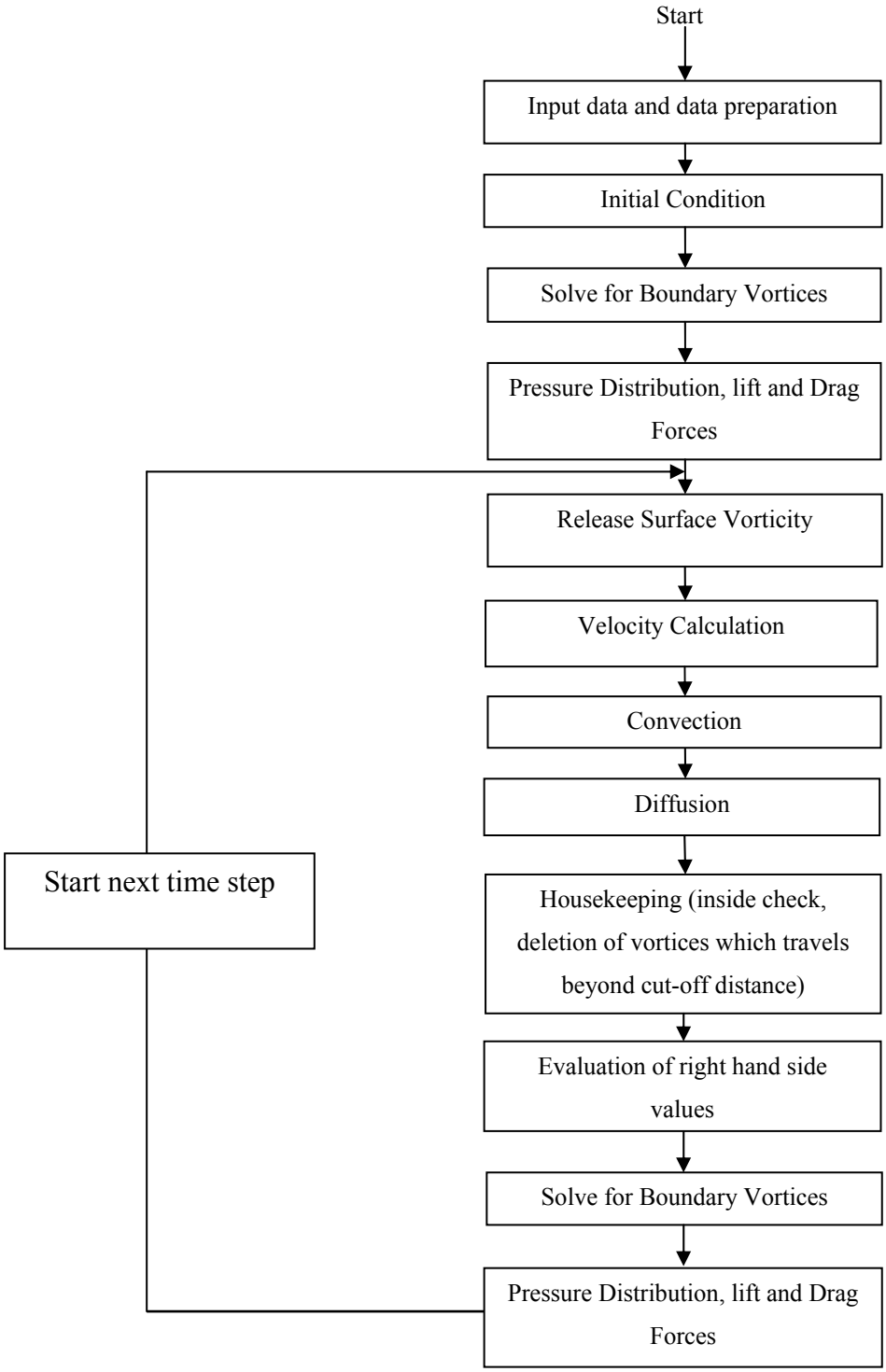

Figure 2-6 Computational scheme of the present study

2.12 Parallelization

In vortex methods, the computational elements are the vortex particles. So, the flow is simulated mainly by calculating the interaction of these particles with each other. In this respect, vortex methods are N-body problems which simulate the evolution of a system of N bodies, where the force exerted on each body arises due to its interaction with all the other bodies in the system. In N body problems, the simulation proceeds over time steps, each time computing the net force on each body and thereby updating its position and other attributes. If all pairwise forces are computed directly, it is called direct method and this requires $O(N^2)$ operations at each time step. So, in direct methods, as the particle number increases in the system the total simulation time increases by square of particle number. This results in high computational cost. However, since solutions of N-Body problems lack of data dependency, these problems are well suited for parallel programming. Because of these reasons, it is decided to apply parallel computations. So, in the current numerical simulation, parallelization is done by using Single Instruction Multiple Data (SIMD) architecture. Moreover, the parallel computation procedure includes the usage of MPI libraries, so the numerical implementation could be used in both distributed and shared memory systems.

In the present study, the parallelization is conducted only for velocity calculation subroutine. Because the main computational effort is spent in this subroutine, as it is figured below (Figure 2-7):

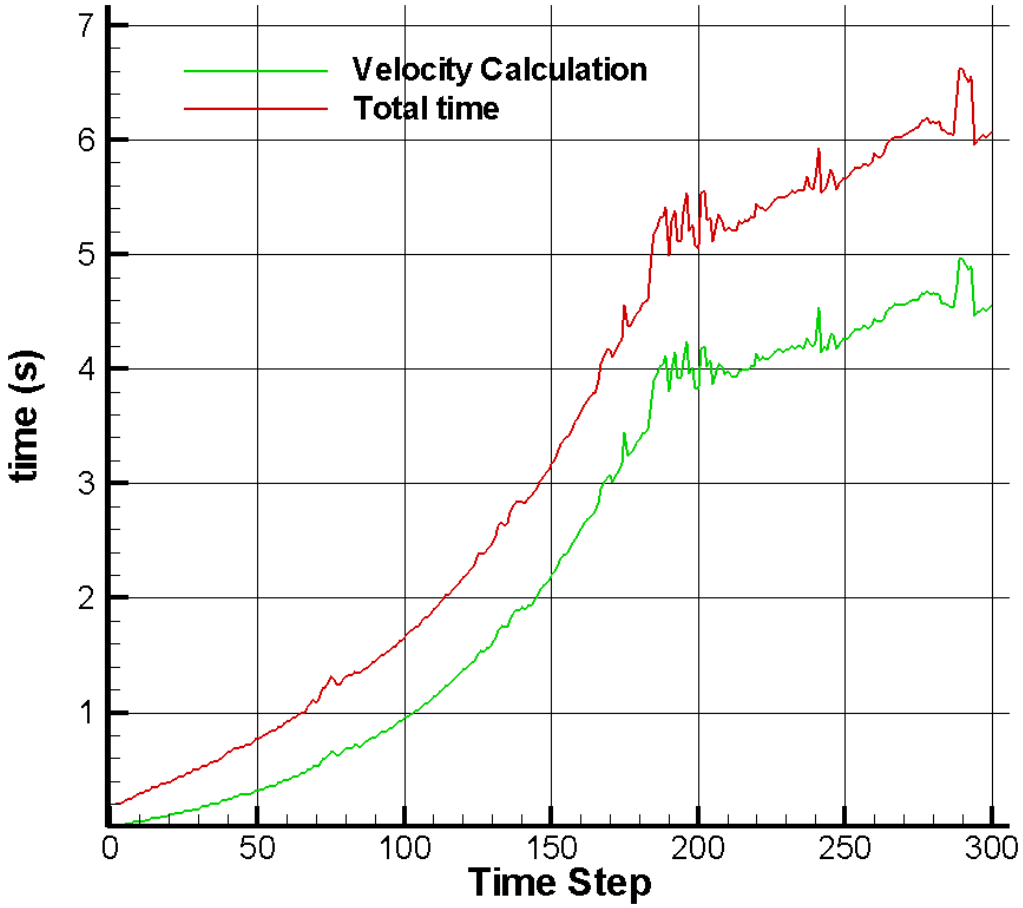

Figure 2-7The required time at each time step for a whole calculations at that time step and only velocity calculation process

At this test case, % 71.3 of total time is spent for velocity calculation process.

2.12.1 Parallel Environment

The parallel computation of present method is carried on a shared memory system (on a workstation computer) for the test case. The computer has two Intel Xeon E5530 2.4 GHz processors each having 4 cores and 24 GB shared memory. The operating system is Microsoft Windows Vista Business.

2.12.2 Parallel Efficiency

As a test case, flow around a bridge section with 200 panels is solved for 300 time steps by using respectively 1, 2, 4, 6 cores of the computer. The speed-up graph is below (Figure 2-8):

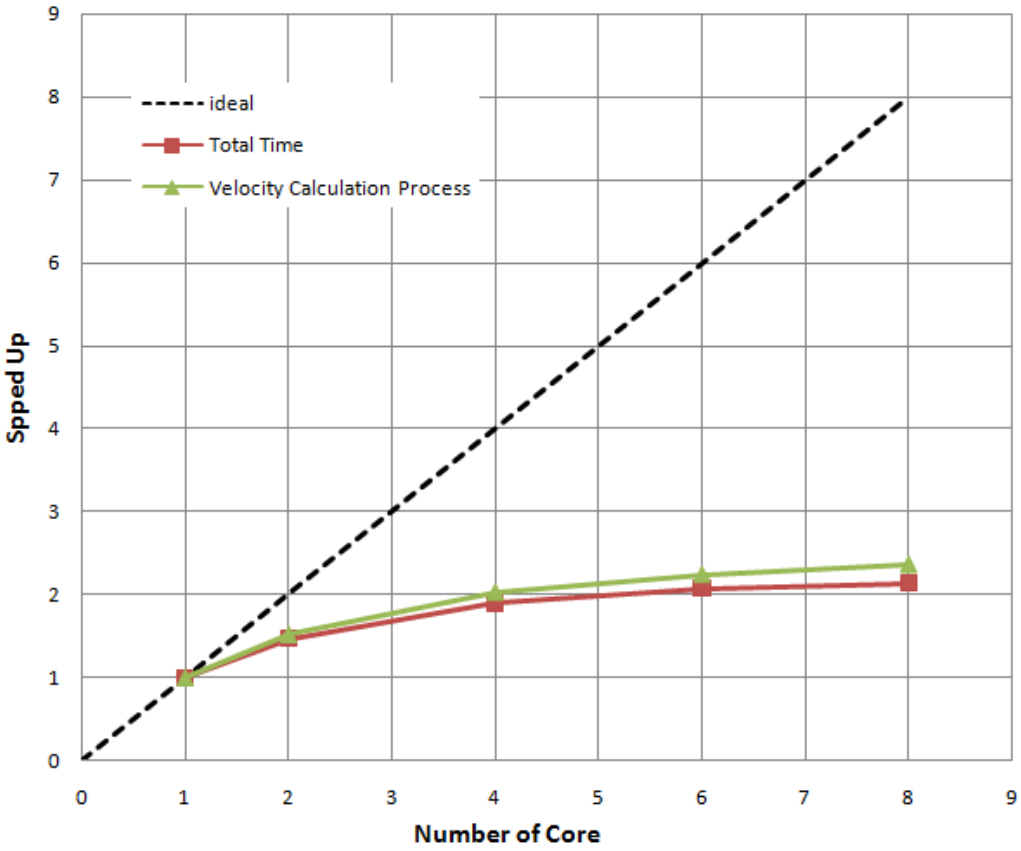

Figure 2-8The speed-up graph of parallel implementation

According to the graph (Figure 2-8), the efficiency of parallelization is not enough. The speed-up limit is found nearly 2.5. Therefore, it is needed to review the parallel implementation.

CHAPTER 3

VALIDATION STUDIES

3.1 Introduction

In this chapter, the case studies performed to verify the numerical implementation are detailed. The case studies are selected as basic unsteady bluff body flow problems, such as a circular and a square cylinder and a NACA 0012 airfoil (since bluff bodies are defined according to the inflow direction, a streamlined body may still be bluff at certain angle of attack). In these case studies, the focus point is to match pressure distribution, wind loads, flow characteristics and Strouhal number, which are important for wind engineering to design a structure, with the experimental data.

3.2 Flow Past A Circular Cylinder

Flow past a circular cylinder is an important and a challenging problem in computational fluid dynamics. This problem is also considered as a standard benchmark problem in the vortex methods community. So that is a good reason to start verifying numerical implementation by solving the problem that flow past a circular cylinder. Another reason for choosing this problem is that for such a flow there is a large amount of experimental data available to check the computations. The test cases are performed for a circular cylinder at Reynolds number 10 000.

The results obtained from the implementation are compared with the experimental data and DNS results. But, first of all to show grid independency, number of panels and grid spacing values are varied and the optimum numerical parameters are fixed.

3.2.1 Selection of Numerical Parameters

To detect optimum values of numerical parameters, such as number of panels, grid spacing values, flow past a circular cylinder at Re 10 000 is solved with different numerical parameters. Then, the results are compared with experimental values.

For the sake of detecting optimum numerical parameters, flow past a circular cylinder is solved for number of panels, N = 60, 120, 200, 300 and grid spacings, Δs = 0.1, 0.05, 0.025 of diameter of the circular cylinder.

3.2.1.1 Selection of number of panels

Firstly, the effect of number of panels on the result is considered. To be able to evaluate the effect of number of panels Δs is held fixed at 0.05 D, and the number of panels is changed to 60, 120, 200, and 300. The results are as following:

Table 3-1 Comparison of cd results of simulations with different numbers of panels and experimental data (Figure 3-10) [58]

Number of panels	Predicted cd value	Experimental cd value	Difference (%)
60	1.4318	≈1.20	19.32
120	1.3567	≈1.20	13.06
200	1.3136	≈1.20	9.47
300	1.3428	≈1.20	11.90

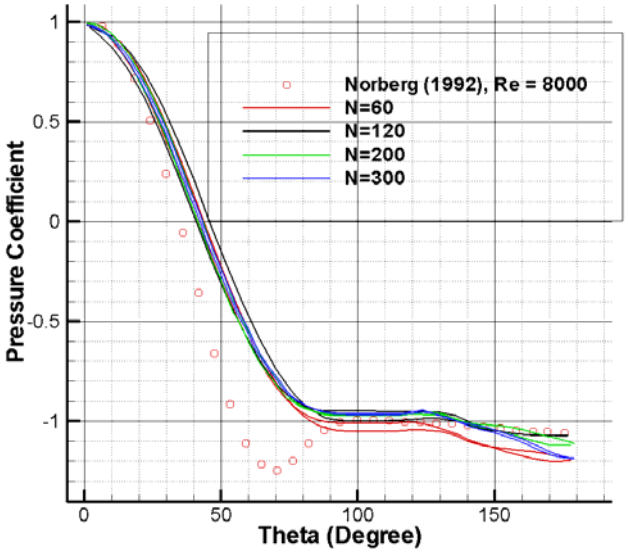

Figure 3-1Comparison of pressure coefficients on cylinder surface between simulation (Re 10 000) with different panel numbers and experimental data, Re 8000 in Norberg [59]

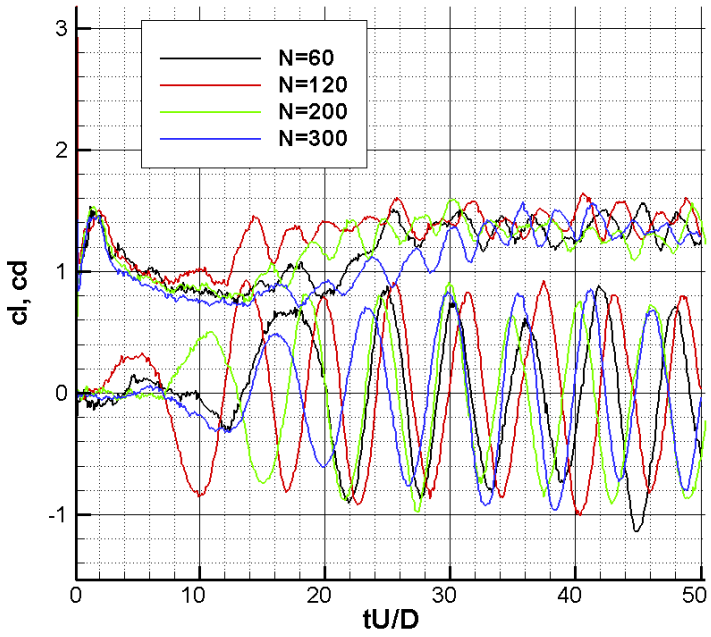

Figure 3-2 Time history of force coefficients of present study around a circular cylinder at Re 10 000 with different panel numbers

Table 3-2 Comparison of present cl r.m.s. results on cylinder surface between simulations with different numbers of panels and experimental value [60]

Number of panels	Predicted cl r.m.s. value	Experimental cl r.m.s value	Difference (%)
60	0.597	0.532	12.22
120	0.568	0.532	6.77
200	0.557	0.532	4.70
300	0.596	0.532	12.03

Table 3-3 Comparison of Strouhal number on cylinder surface between simulations with different numbers of panels and experimental values (Figure 3-11) [60, 61, 62]

Number of panels	Predicted Strouhal number	Experimental Strouhal number	Difference (%)
60	0.166	≈ 0.2	17.00
120	0.176	≈ 0.2	12.00
200	0.196	≈ 0.2	2.00
300	0.188	≈ 0.2	6.00

According to analyses done with different number of panels, it is concluded that selection of number of panels affects the results for force and vortex shedding frequency values. Moreover, it could be said that increasing number of panels improves accuracy of simulation up to a point. For the present results for flow past a circular cylinder simulation, '200' is considered the optimum number for number of panels.

3.2.1.2 Selection of grid spacing

After deciding the number of panels, to decide the optimum grid spacing value, simulation of flow around a circular cylinder at Re 10 000 is performed for variant grid spacing values (h) with 200 panels. The results are as following:

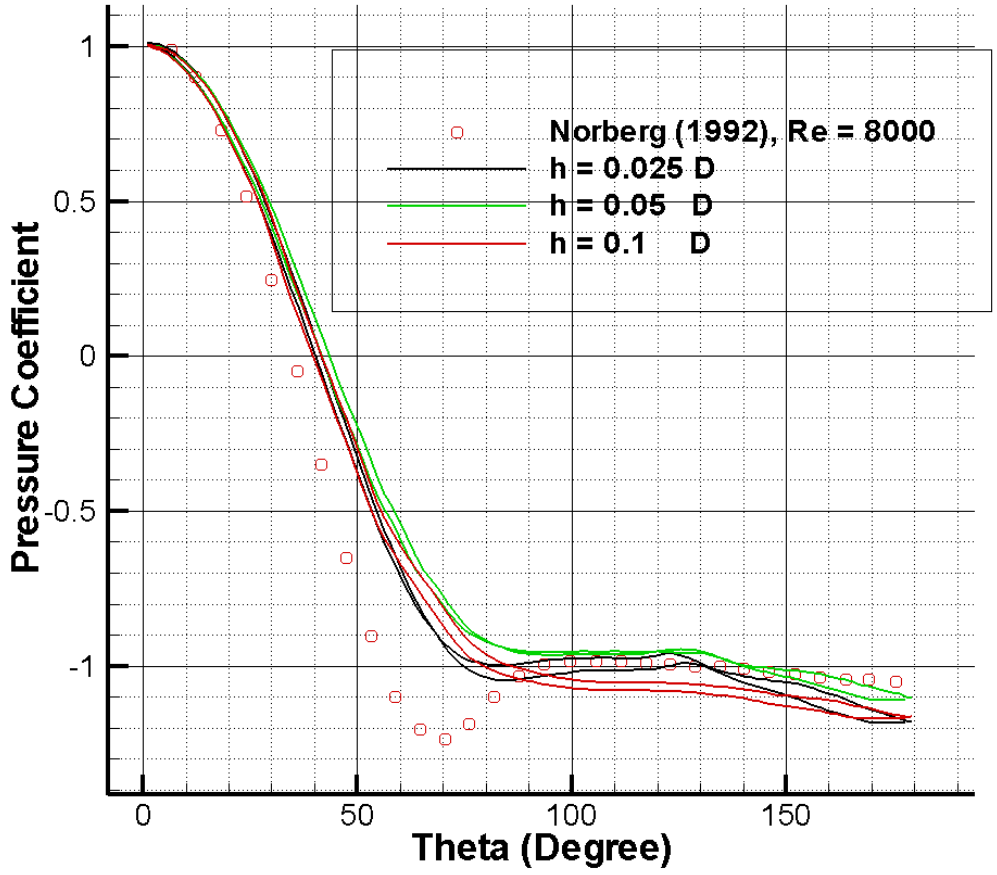

Figure 3-3Comparison of pressure coefficients on cylinder surface between simulation (Re 10 000) with different panel numbers and experimental data, Re 8000in Norberg [59]

Table 3-4 Comparison of present cd results on cylinder surface between simulations with different numbers of panels and experimental values (Figure 3-10) [58]

Grid Spacing (D)	Predicted cd value	Experimental cd value	Difference (%)
0.1	1.2987	≈ 1.2	8.23
0.05	1.3136	≈ 1.2	9.47
0.025	1.2625	≈ 1.2	5.21

Table 3-5 Comparison of present cl r.m.s. results on cylinder surface between simulations with different numbers of panels and experimental values [60]

Grid Spacing (D)	Predicted cl r.m.s. value	Experimental cl r.m.s value	Difference (%)
0.1	0.530	0.532	0.38
0.05	0.557	0.532	4.70
0.025	0.583	0.532	9.84

Table 3-6 Comparison of Strouhal number on cylinder surface between simulations with different numbers of panels and experimental values (Figure 3-11) [60, 61, 62]

Grid Spacing (D)	Predicted Strouhal number	Experimental Strouhal number	Difference (%)
0.1	0.179	≈ 0.2	10.50
0.05	0.196	≈ 0.2	2.00
0.025	0.174	≈ 0.2	13.00

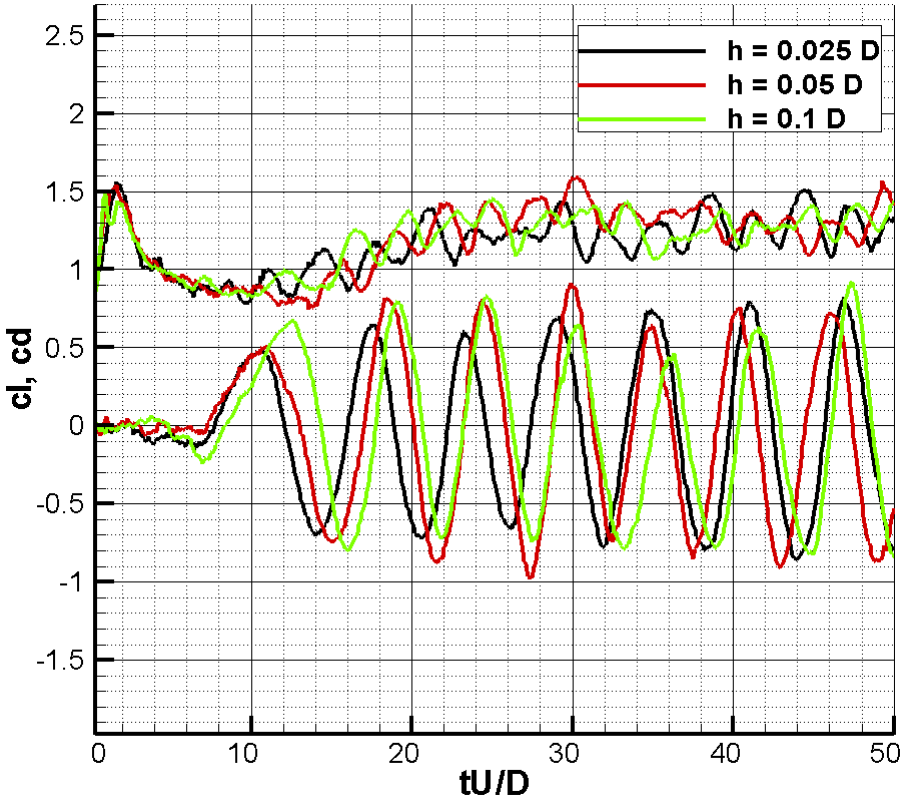

Figure 3-4 Time history of force coefficients of present study around a circular cylinder at Re 10 000 with variant grid spacing

According to the results for pressure coefficient distribution, the simulation with h=0.1 D under-predicts the base pressure, but the simulations with h=0.05 and h=0.025 D predict the base pressure value better according to the results. Moreover, the best results is obtained with h=0.05 D.

When force coefficients are considered, drag coefficient is best predicted with grid space size, h=0.025 D. On the contrary of drag coefficient, lift coefficient root mean square value is best predicted with grid space size, h=0.1 D.

Finally, Strouhal number is best predicted with grid space size of h=0.05 D. So it is hard to say that the solution is better with finer grid among the experienced grid space sizes. As a consequence, it is decided to use 0.05 D grid spacing that gives the closest Strouhal number which is important to get accurately for wind engineering problems. So, the analyses conducted after that is performed with these parameters (200 number of panels and 0.05 D grid spacing).

3.2.2 Flow past a circular cylinder at Re 10 000

After deciding the numerical parameters, flow past a circular cylinder at Re 10 000 is solved for longer time. Then the results that are obtained for longer time are compared with results of experiment of Norberg [59] and DNS of Karniadakis *et. al.* [64].

3.2.2.1 Flow Patterns

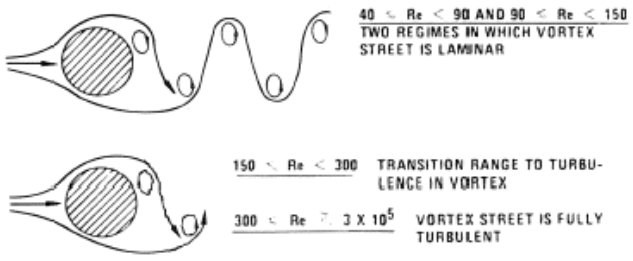

Figure 3-5 Flow patterns for circular cylinder at different Reynolds number [65]

There should be a laminar separation at Re 10 000, on the surface of circular cylinder and there should be a Karman Vortex Street which is fully turbulent. So,

it is expected from numerical simulation that the separation point should be predicted accurate, and the obtained vortex shedding frequency should be close to DNS results.

Figure 3-6 Flow around a circular cylinder at non-dimensional time 100 for Re 10 000

From the figure (Figure 3-6), it could be seen that the numerical implementation captured the vortex street well for both cases. To compare the vortex shedding frequency and separation points, Strouhal number and pressure coefficient distribution should be obtained.

3.2.2.2 Pressure Coefficients

Firstly, mean pressure coefficient distribution on the circular cylinder surface is compared with the experimental data by Norberg [59] at Re 8000.

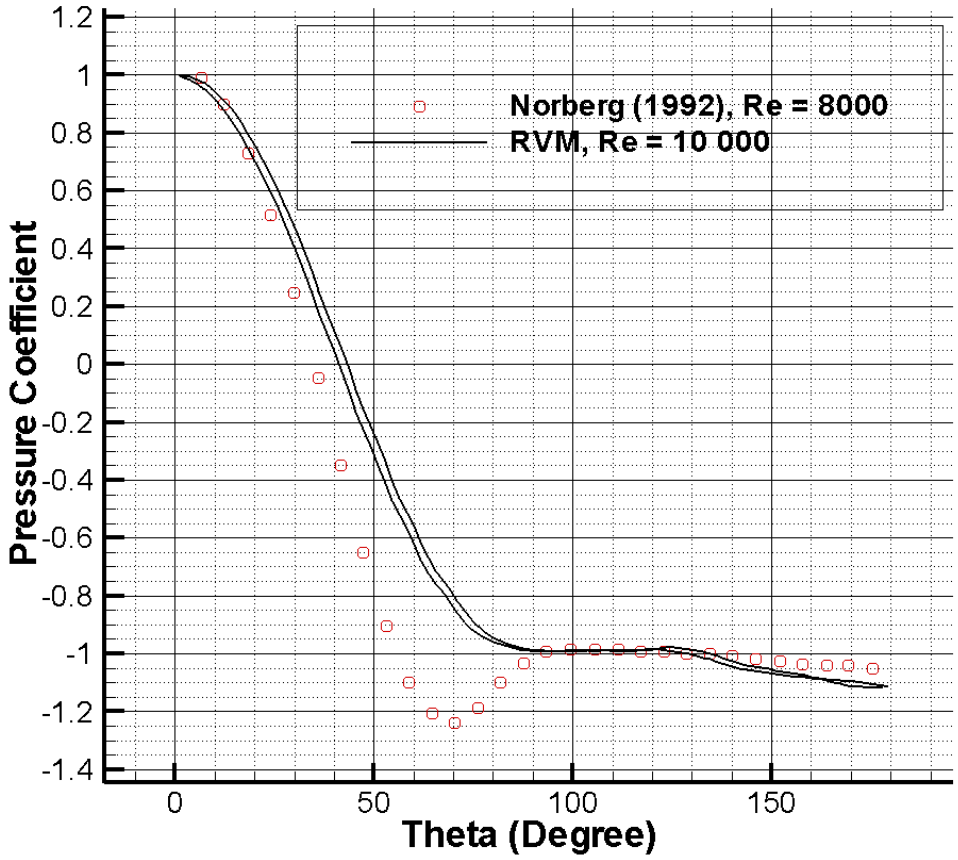

Figure 3-7 Comparison of pressure distribution around a circular cylinder of present study with Norberg experiment [59].

According to graph (Figure 3-7), quite reasonable results are obtained which is well-matched with experimental data. Especially, base pressure value of simulation exhibits a good agreement with experimental value. Although, the numerical simulation found the separation point slightly further downstream. Moreover, in the region that upstream of separation, the accelerating potential flow is predicted slower. This is arguably because of that RVM over-predicts minimum pressure, so the potential flow accelerates slower.

3.2.2.3 Force Coefficients

The comparisons for the fluid flow around a circular cylinder case are made also with force data (Figure 3-8, Figure 3-9). It should be noted that, the forces calculated with RVM is obtained by considering only pressure forces, so viscous forces are neglected. But this is a reasonable assumption, since for bluff bodies the dominant force is the pressure force. The results obtained for Re 10 000 are figured and tabulated at following tables (Table 3-7, Figure 3-8);

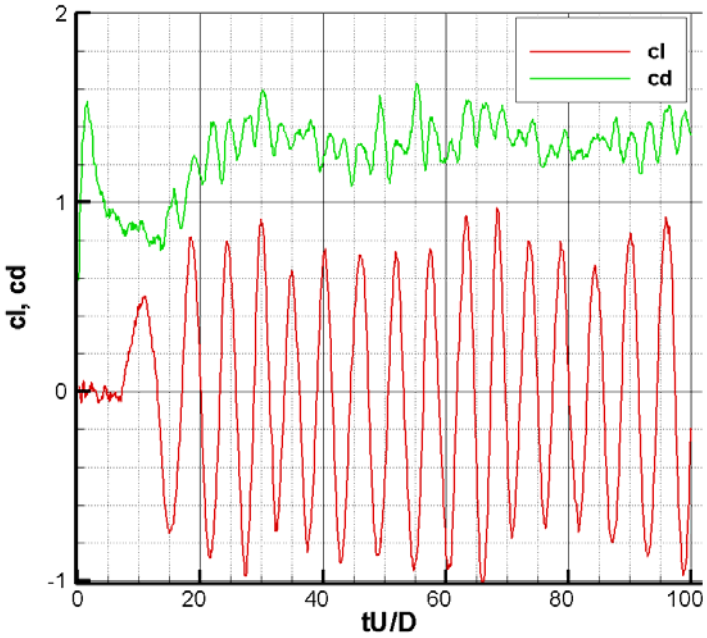

Figure 3-8 Time history of force coefficients of present study around a circular cylinder at Re 10 000

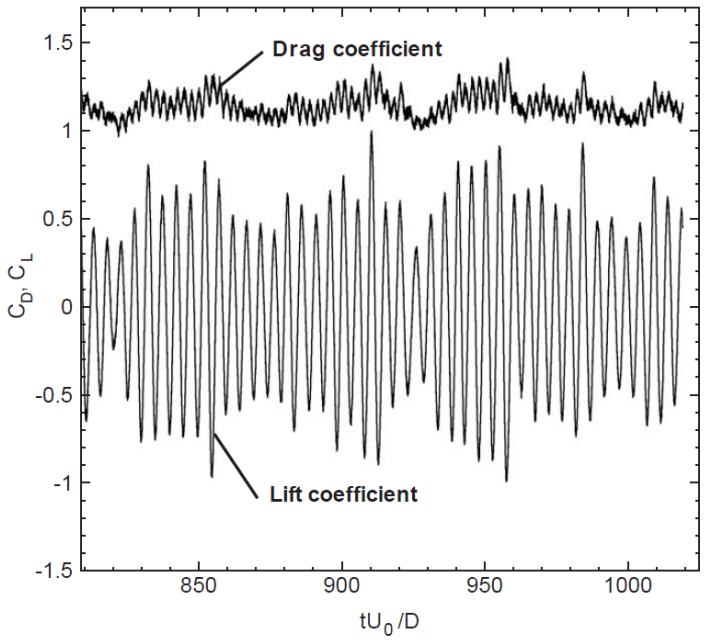

Figure 3-9 Time history of force coefficients of DNSof uniform flow past a circular cylinder at Re 10 000 [64]

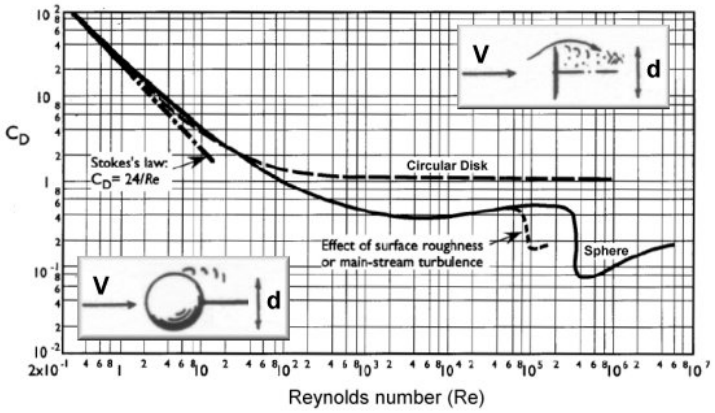

Figure 3-10 Drag coefficient of a circular disk and a sphere versus Reynolds number [58]

Table 3-7 Comparison of force coefficient values of the present results with experimental values and DNS results

Case	cd	cl r.m.s
RVM	1.325	0.573
Experimental results [58]	≈ 1.2	-
Moeller and Leehey [60]	1.186	0.532
*DNS - B1 [64]	1.208	0.547
*DNS - B2 [64]	1.120	0.497
*DNS - B3 [64]	1.143	0.448

* B1, B2, B3 mean analyses done with different resolutions at the paper [64]

According to the results, the numerical implementation over-predicts drag coefficient value. This is surely, because of inability to catch minimum pressure value. Although, cl r.m.s. value is in a good agreement with experimental value.

3.2.2.4 Vortex Shedding Frequency

The vortex shedding frequency is an important design parameter for structures Therefore, to predict the accurate vortex shedding frequency is challenging and important. The dimensionless parameter which describes the shedding frequency is the Strouhal number;

$$St = fL/V \tag{2.23}$$

Where St is Strouhal number, f is the shedding frequency and V is free stream flow velocity. In this study, the Strouhal numbers are calculated and compared with experimental data (Figure 3-11) and DNS results.

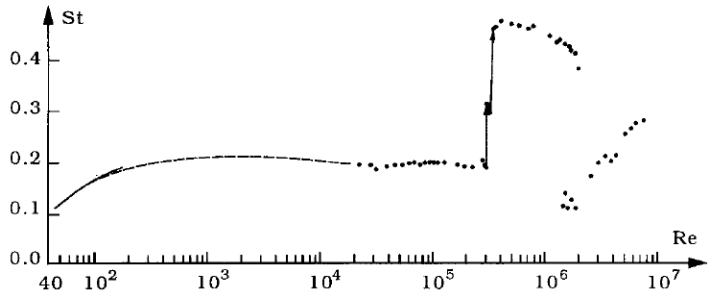

Figure 3-11 Strouhal number for a smooth circular cylinder. Experimental data from: Solid curve: Williamson [61]. Dashed curve: Roshko [62]. Dots: Schewe [63]

The frequency of vortex shedding which are obtained with the numerical simulations, are calculated by using lift coefficient oscillations. By taking discrete Fourier transform of lift oscillations, between dimensionless time 20-90 for Re 10 000, where complete fourteen oscillation cycles are completed, the frequencies of vortex shedding are calculated (Figure 3-12). Then, the dominant frequencies are averaged according to their amplitude, so Strouhal number is obtained.

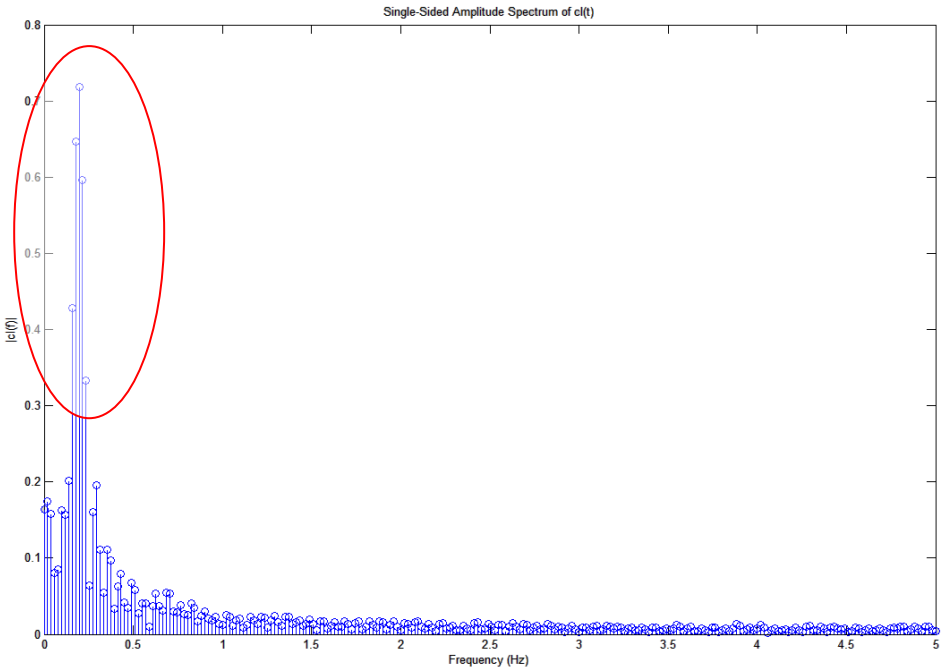

Figure 3-12 Discrete Fourier transformation result of lift oscillation of analysis around a circular cylinder at Re 10 000

The results of numerical simulations and their comparisons with experimental data are tabulated at following table (Table 3-8).

Table 3-8 Comparison of Strouhal number that obtained from present study around a cylinder at Re 10 000 with experimental data

Case	Strouhal Number
RVM	0.195
Experiment [61], [62], [63]	≈ 0.2
DNS - B1 [64]	0.200
DNS - B2 [64]	0.205
DNS - B3 [64]	0.203

Actually, the obtained results are in very good agreement with the experimental value and DNS results. So, the results are encouraging to simulate wind engineering problems, in which vortex shedding frequency is an important parameter.

Hence, the results clearly show the ability of the numerical implementation to simulate flow around a circular cylinder.

3.3 Flow Past A Square Cylinder

As a first test case, flow around a circular cylinder is selected, whereas, from engineering point of view, it is also necessary to investigate flow around different bluff body shapes, such as a shape with sharp edge corners. So as a second test case, the fluid flow around a square is studied. The analysis is performed at Re 20 000. The reason for choosing Re 20 000 is that there is available experimental and numerical results for the square cylinder at this Reynolds number. So, the calculated results are compared with these experimental and numerical values.

3.3.1 Flow Patterns

At Re 20 000, it is expected that there is a strong vortex shedding. So the flow is characterized by a Karman vortex street, which is formed from vortices that in a regular alternating arrangement. Moreover, the separation should occur from upstream corners.

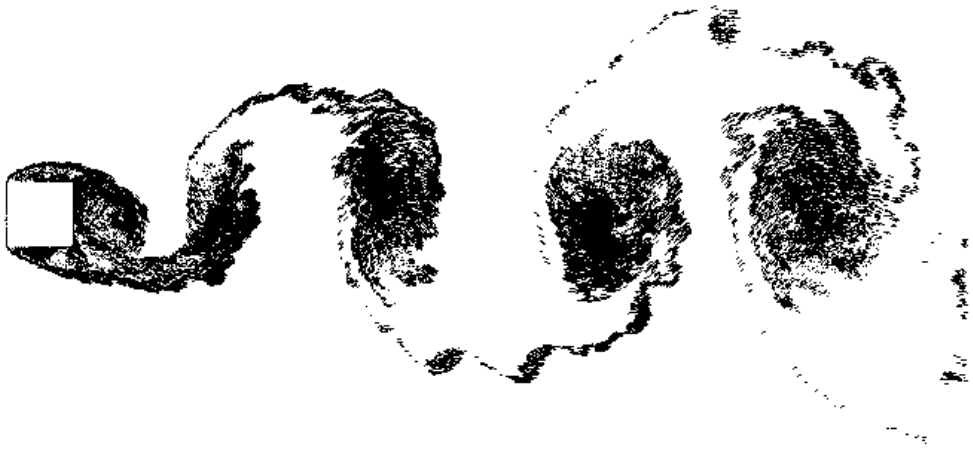

Figure 3-13 Flow around a square cylinder at non-dimensional time 30 for Re = 20 000

The flow pattern at dimensionless time 30 is shown at figure (Figure 3-13). From the figure (Figure 3-13), the regular vortex shedding and the separation at upstream could be seen clearly.

3.3.2 Pressure Coefficients

The comparison of pressure coefficients are made with the experimental results [66]. The comparison is at the following figure (Figure 3-14);

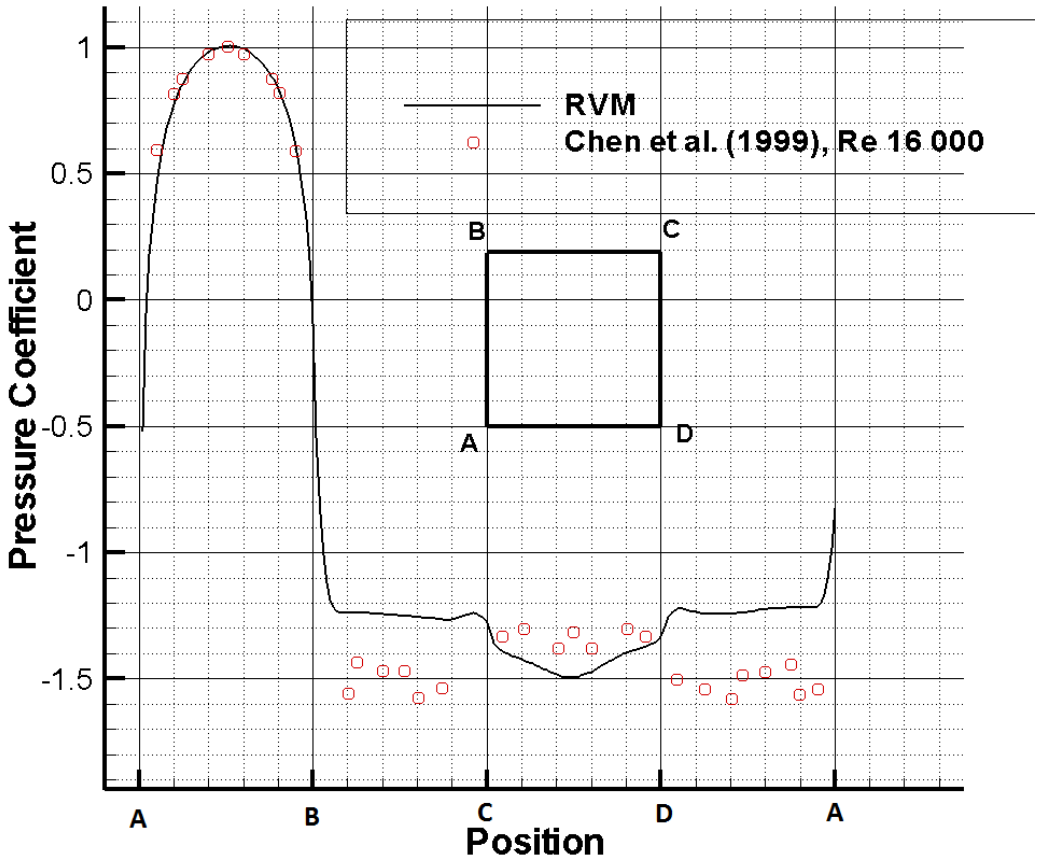

Figure 3-14 Comparison of present results around a square cylinder at Re 20 000 with experimental result of Chen *et al.* [66]

When the results of pressure coefficients are compared, it is seen that the pressure coefficients for the upstream flow edge is well matched (Figure 3-14). Moreover, it is obvious from the pressure distribution, in both cases, flow separation occurs at upstream corners. Furthermore, base pressure value is predicted well, when it is compared with experimental value. However, as it was also seen in the simulation of the flow around a circular cylinder, potential flow isn't able to accelerate enough and for this reason between A-D and between B-C pressure coefficient is over-predicted.

3.3.3 Force Coefficients

The comparisons of results are made again with the experimental data (Figure 3-16). The force coefficients are calculated between non-dimensional time 22-99, where eleven complete oscillations is completed. The time history of coefficients and experimental results are figured below (Figure 3-15, Figure 3-16);

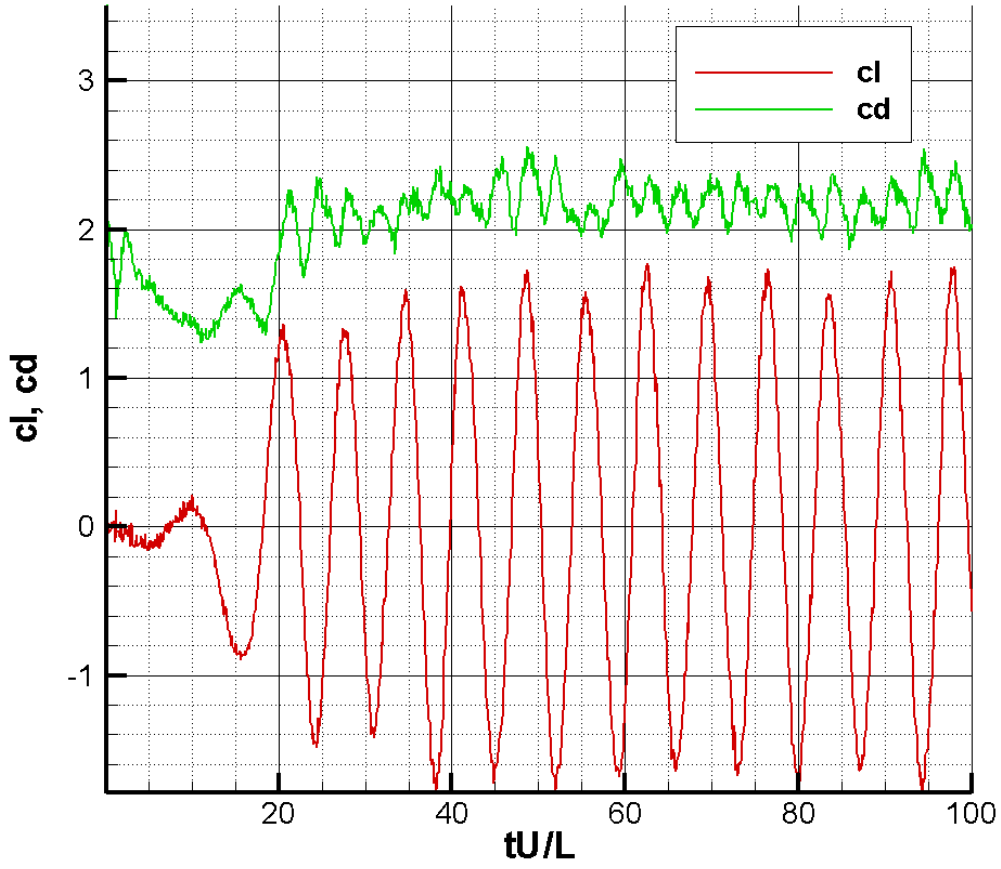

Figure 3-15 Time history of force coefficients of present study around a square cylinder at Re = 20 000

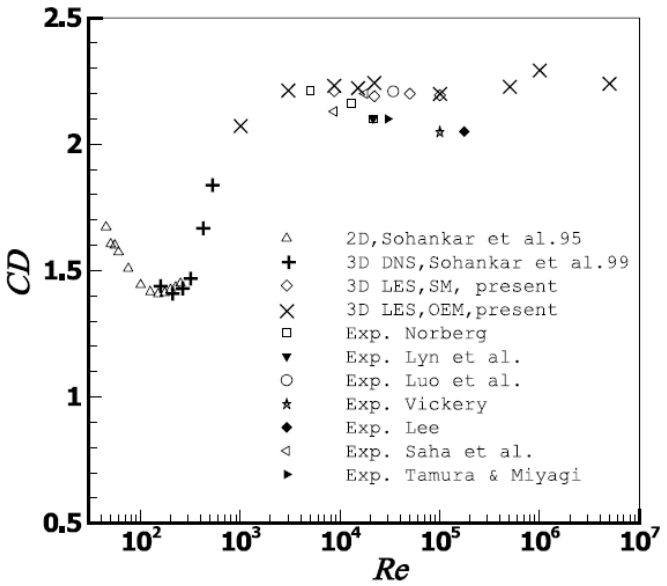

Figure 3-16 Experimental [67], [68], [69], [70], [71], [72], [73]and numerical [74], [75] drag coefficient values at different Re

Table 3-9 Comparison of the present result of drag coefficient at Re 20 000 with experimental value in literature (Figure 3-16)

Re	RVM	Experimental	Difference (%)
20 000	2.1696	≈2.15	1.0

The difference between drag coefficient value of the present simulation and experimental value is around % 1, which is acceptable from an engineering point of view.

Root mean square lift coefficient of the simulation is compared with some numerical values. The comparison is at following table:

Table 3-10 Comparison of lift coefficient root mean square value of the present simulation of flow around a square cylinder at Re 20 000 with some numerical results [76], [77]

Reference	Numerical Method	cl r.m.s
Present Simulation	Vortex Methods	1.11
Wang and Vanka [76]	LES	1.29
Porquie *et. al.* [77]	LES	1.01, 1.02, 1.12

According to the results (Table 3-10), the cl r.m.s value is in a good agreement with numerical results.

3.3.4 Vortex Shedding Frequency

To detect Strouhal number, again time history of lift coefficient is used. Discrete Fourier transform of lift coefficient is calculated to obtain frequency (Figure 3-17).

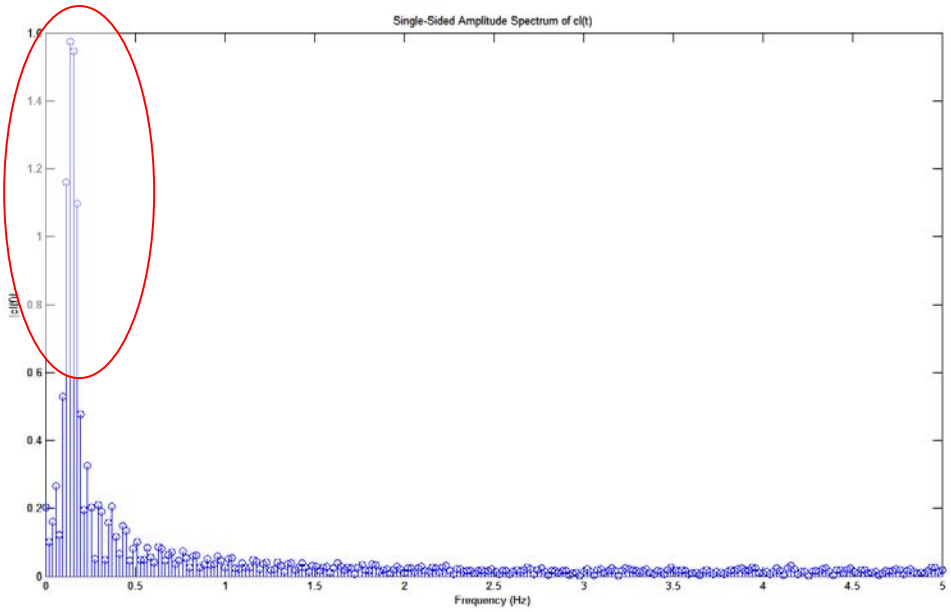

Figure 3-17 Discrete Fourier transformation result of lift oscillation of analysis around a square cylinder at Re 20 000

The comparison of Strouhal number is made with experiment of Lyn*et.al*. [78], [79]. The results are tabulated below (Table 3-11);

Table 3-11 Comparison of Strouhal number obtained from present study of flow around a square cylinder at Re 20 000 with experimental result of Lyn *et. al.* [78], [79]

Re	RVM	Lyn*et. al.*[78], [79]	Difference (%)
20 000	0.145	0.132	9.8

3.4 Flow Past NACA 0012 airfoil at angle of attack 20^0

To show capabilities of random vortex methods to solve separated flows, flow past NACA 0012 airfoil simulation at angle of attack 20^0 is conducted with current numerical implementation.

3.4.1 Flow Patterns

At large angles of attack, there is a flow separation around NACA 0012 airfoil which occurs close to the leading edge and there occurs a large recirculation zone above the airfoil surface. Moreover, large vortices which shed from leading edge intermittently formed. Therefore, it is expected from the present solver to capture these large vortices and the recirculation zone that is above the airfoil surface.

Figure 3-18 Flow around NACA 0012 airfoil at non-dimensional time 20 for Re = 10 000, at angle of attack 20^0

It could be seen from the figure (Figure 3-18), large vortices which shed from leading edge formed intermittently, and there is a recirculation zone above the

airfoil. So, the present study gives the main features of the flow around NACA 0012 airfoil at 20^0 of angle of attack.

3.4.2 Pressure Coefficients

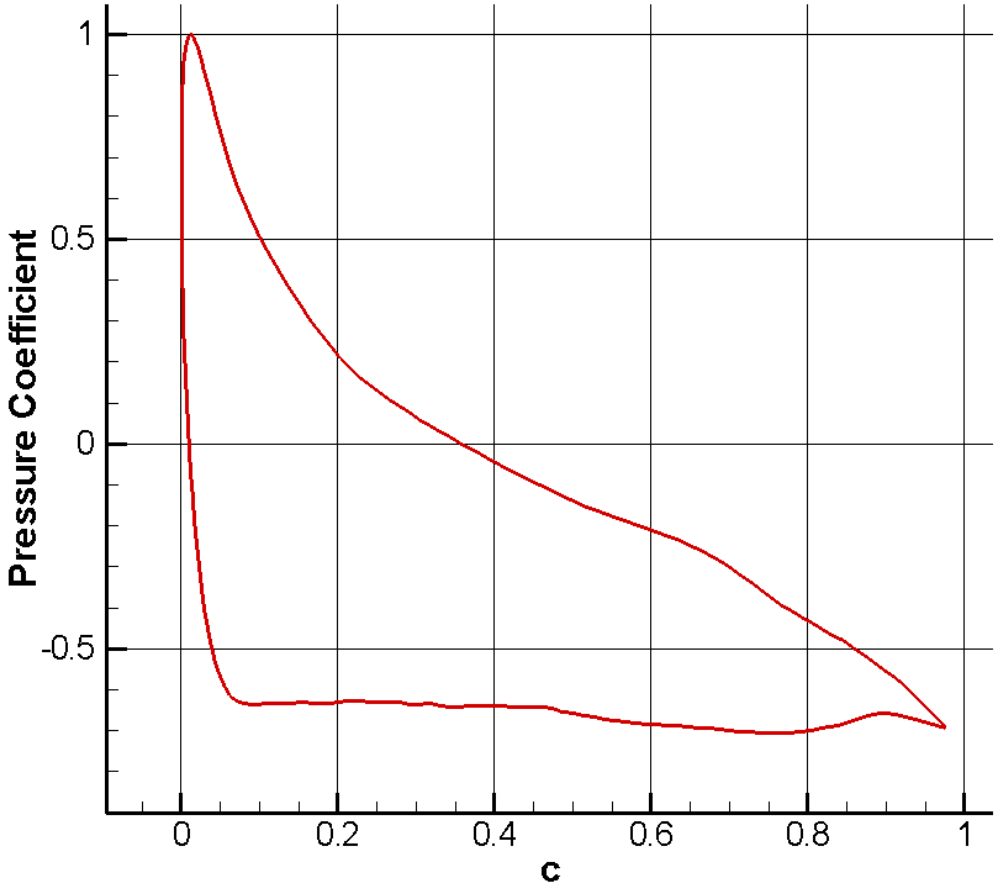

Figure 3-19 Calculated mean pressure coefficient pressure distribution around NACA 0012 airfoil at Re 10 000 and at 20^0 angle of attack

From the figure (Figure 3-19), the separation from the leading edge could be seen clearly. Moreover, the effect of trailing edge vortex which rolls up unsteadily to the upper surface could be seen as an increase in pressure coefficient, after chord

length of 0.8. On the contrary of upper surface, on the lower surface, where flow is always attached, flow is accelerated, so the pressure decreases steadily.

3.4.3 Force Coefficients

The separation, which causes intermittently formed large vortices, leads to an alternating pressure distribution, hence changes in lift coefficient value with time. On the contrary of lift coefficient, the oscillations in drag coefficient is smaller, furthermore the oscillations in drag coefficient is coherent with lift oscillations. So, this entire phenomenon could be seen from the time history of force coefficient, which is obtained from present study (Figure 3-20).

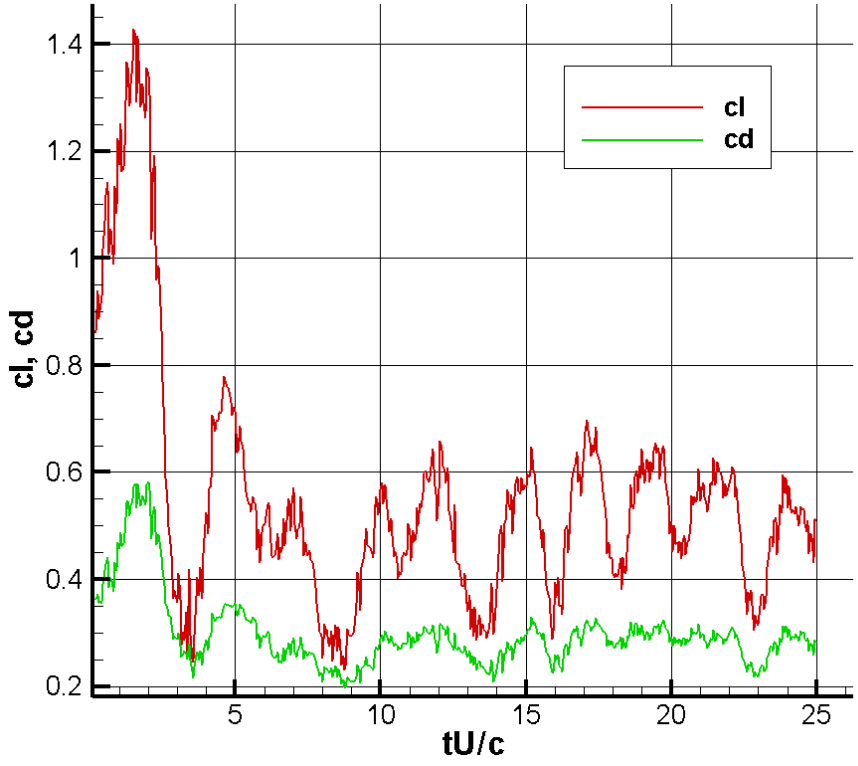

Figure 3-20 Time history of force coefficient of present study for flow around NACA 0012 airfoil at angle of attack 20^0 and Re 10 000

Moreover, the comparison of mean force coefficient values with experimental data [80] is conducted and a fairly good agreement with experimental results is seen.

Table 3-12 Comparison of force coefficient of present simulation results with experimental results [80]

Reference	cl	cd
Present Simulation	0.513	0.2816
Experiment [80]	0.584	0.2970

3.5 Flow Past an Oscillating Circular Cylinder at Re 10 000

In this section, flow past a circular cylinder experiencing a forced oscillation with the frequency 0.21 Hz, and displacement amplitude 0.3 D. The emphasis is put on the influence of forced oscillation on only force coefficients. The comparisons are made with both numerical and experimental results.

3.5.1 Force Coefficients

The comparisons of results are conducted with the experimental and numerical results (Table 3-13).

Table 3-13 Comparison of force coefficient of present simulation results with experimental and numerical results

Reference	cl magnitude	cd
Present Simulation	1.4752	1.881
Gopalkrishnan [81], Exp.	≈1.29	≈1.65
Karniadakis *et. al.* [64], DNS	≈1.23	≈1.51

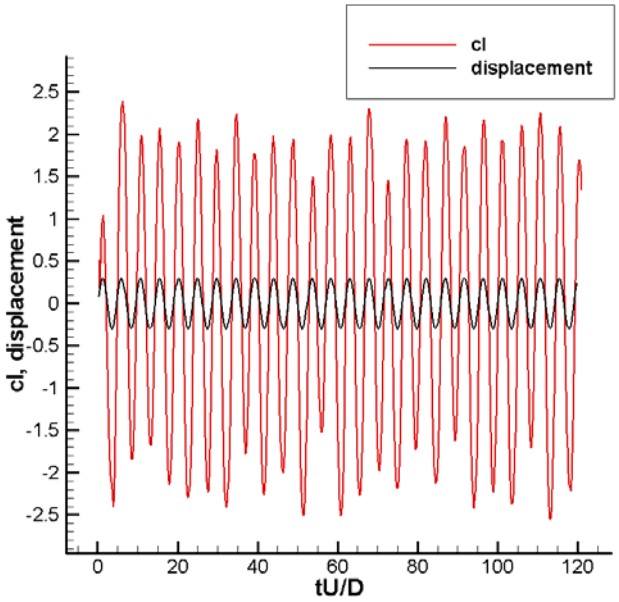

Figure 3-21 Time history of lift coefficient and cylinder displacement in flow past an oscillating cylinder at Re= 10 000; oscillation frequency fD/U=0.21; Y/D=0.3, Present simulation

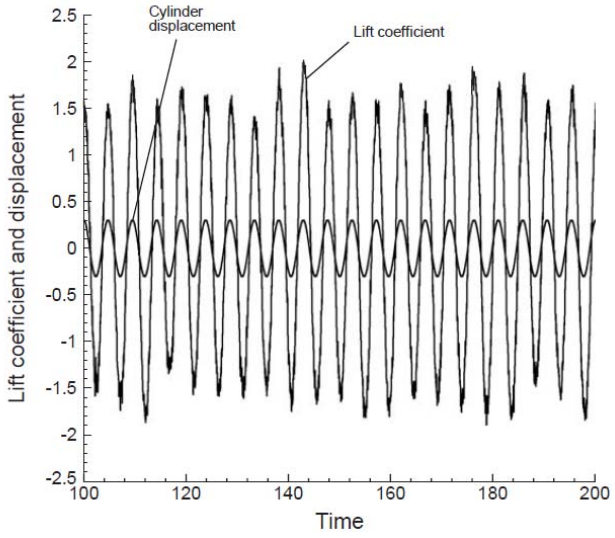

Figure 3-22 Time history of lift coefficient and cylinder displacement in flow past an oscillating cylinder at Re= 10 000; oscillation frequency fD/U=0.21; Y/D=0.3, DNS [64]

The simulation has captured dramatic increase in oscillation amplitude of lift coefficient, but it over-predicts the value. Moreover, the lift force of the simulation oscillates at the cylinder oscillation frequency (Figure 3-21) which is also the case for DNS [64] (Figure 3-22). The present simulation gives moderate change in drag coefficient as DNS [64] and experiment [81]. However, the simulation again over-predicts the value of drag coefficient. Despite over-prediction of force coefficients (around % 10), the simulation has captured main features of flow around an oscillating cylinder at Re 10 000.

Having shown the applicability of random vortex method based parallel solver to bluff body aerodynamics problems, it is performed to solve flow around long span bridge cross section.

CHAPTER 4

AERODYNAMIC ANALYSIS OF LONG-SPAN BRIDGE CROSS-SECTIONS

4.1 Introduction

In this chapter, the developed numerical implementation will be used to deal with an important computational wind engineering problem that flow over long-span bridge section. Since the vortex-induced forces acting on the bridge section is important, the random vortex method is a suitable technique to analyze a bridge section. So, here the method is applied to a bridge section which is a trapezoid section with B/D ratio 15. Moreover the results that obtained from analysis will be compared with the experimental and numerical data, which are obtained by Uzol & Kurç [82]

The validation study of square section cylinder (generally rectangular section cylinder) best applies to the shape of long-span bridge decks." In regard to these cylindrical bodies, it is widely recognized that their width-depth ratio B/D strongly affects the characteristics of the separated shear layer that is generated at the leading edge [83]. From this point of view, such sections are classified into two categories, namely, the "separated-type" sections(compact cross sections) and the "reattached type" sections (elongated cross-sections) [84]. The former are generally prone to Karman-type vortex shedding, whereas the latter present more complex phenomena, such as discontinuities in Strouhal number at B/D = 2.8 and

B/D = 6 or the double mode in the lift fluctuations due to unsteady reattachment of the separated shear layer on the side surfaces at 2.0 <B/D < 2.8 [85]. Likewise, most of the bridge decks are quite elongated (B/D ≈ 7) so that occurrence of a reattached shear layer calls for a proper evaluation of other characteristics of the flow, such as the extent of the separation bubble, the convection of the vortices along the surfaces of the deck, and the interaction between vortices shed from the windward and leeward edges [86]." [87]. Since B/D ratio of the investigated bridge section is 15, it is a reattached type section.

4.2 Problem Definition

The geometrical properties of the analyzed trapezoidal bridge section are as followed:

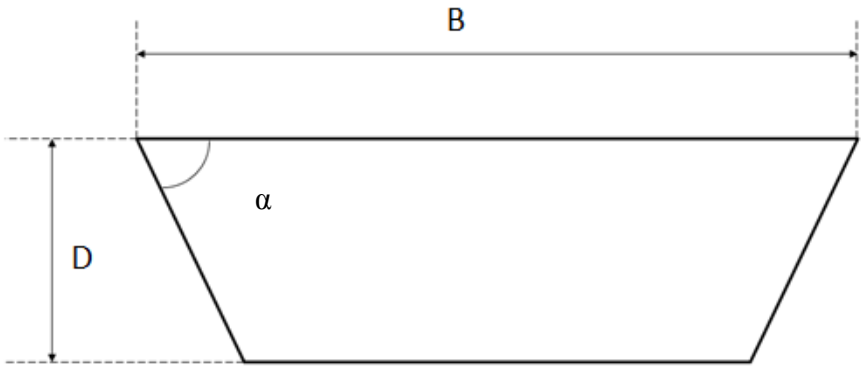

Figure 4-1 Trapezoidal bridge section

Width (B) = 1 m
Height (D) = 0.0666 m
Width/Height (B/D) ratio = 15
Side Angle (α) = 45^0

Analyses are conducted at the same conditions (Table 4-1) with the experiments of Uzol & Kurç [82] (for bridge section of aspect ratio 15 at 5.5 m/s, 9.5 m/s and 14 m/s velocities). The results are compared with the experimental and numerical results which are given in his report [82].

Table 4-1 The flow conditions that is used flow past a long span bridge section analyses

AR	U [m/s]	Re #
15	5.5	1.16E+04
15	9.5	1.97E+04
15	14.0	3.00E+04

4.3 Flow Pattern

Figure 4-2 Flow pattern for the velocity 5.5 m/s at non-dimensional time 10

Figure 4-3 Flow pattern for the velocity 9.5 m/s at non-dimensional time 10

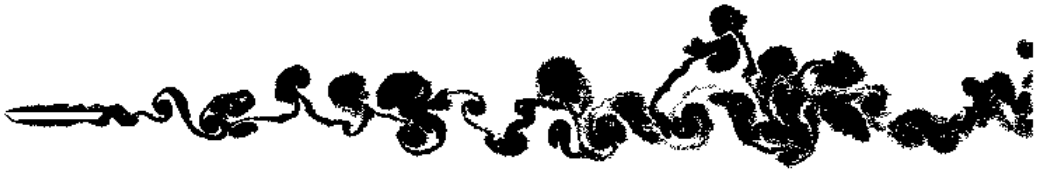

Figure 4-4 Flow pattern for the velocity 14 m/s at non-dimensional time 10

Over the bridge section unsteady re-attachment of separated shear layer is observed. Therefore, the wake is consisted of the vortices that shed unsteadily from upstream and downstream corners. So, an irregular vortex shedding is observed (as it is expected for reattached type sections), as it could be seen from the figures (Figure 4-2, Figure 4-3, Figure 4-4).

4.4 Force Coefficients

The force coefficients were compared with the experimental and numerical data. The time histories of force coefficients that were obtained from the numerical analysis are illustrated at the figures (Figure 4-5, Figure 4-6, Figure 4-7):

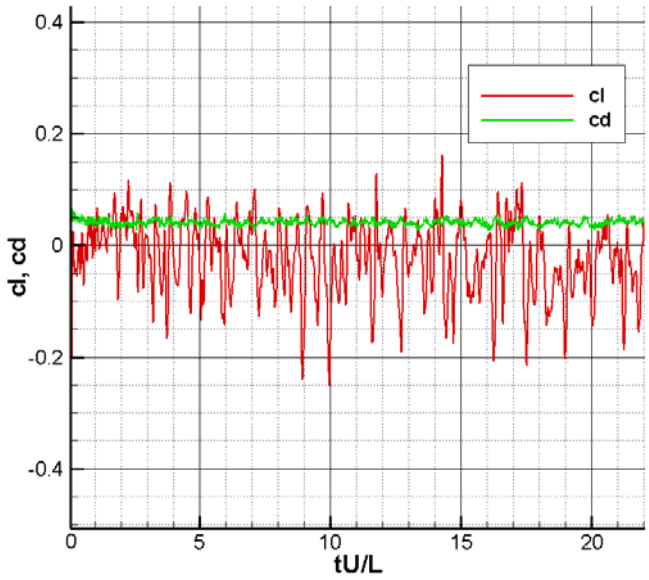

Figure 4-5 Time history of force coefficients of bridge section at velocity 5.5 m/s

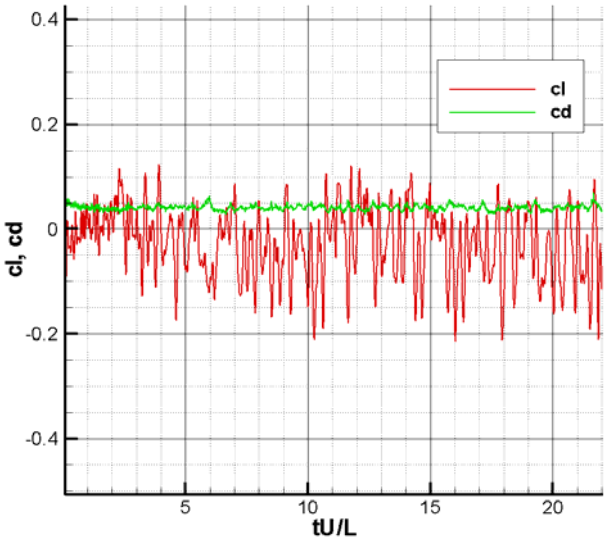

Figure 4-6 Time history of force coefficients of bridge section at velocity 10 m/s

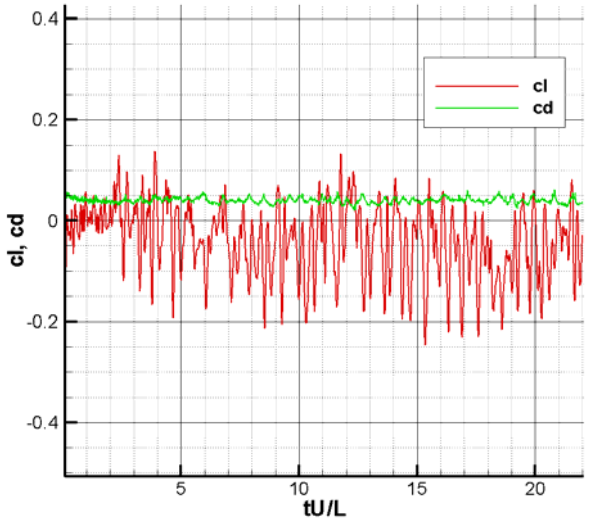

Figure 4-7 Time history of force coefficients of bridge section at velocity 15 m/s

When the time histories of force coefficients are evaluated, it is seen that the drag coefficient values are almost constant with time, there is only small oscillations which is in harmony with lift oscillations. Lift coefficient values represent oscillations which are not regular. Actually, it is an expected attribute, since there is observed unsteady re-attachments of shear layer. The comparison of the calculated values with experimental and numerical data is illustrated below (Table 4-2, Table 4-3):

Table 4-2 Comparison of lift coefficient results of RVM with experimental values

Velocity (m/s)	Experimental	URANS*	RVM
5.5	-0.035	-0.049	-0.031
9.5	-0.045	-0.051	-0.033
14.0	-0.047	-0.049	-0.046

*URANS values are gotten by interpolation

Table 4-3 Comparison of drag coefficient results of RVM with experimental values

Velocity (m/s)	Experimental	URANS*	RVM
5.5	0.030	0.055	0.0411
9.5	0.034	0.054	0.0413
14.0	0.030	0.054	0.0404

*URANS values are gotten by interpolation

According to results, lift coefficient values of present simulation are close to numerical and experimental data.

4.5 Vortex Shedding Frequency

The last comparison is made for Strouhal numbers. The results are as following (Figure 4-8, Figure 4-9, Figure 4-10);

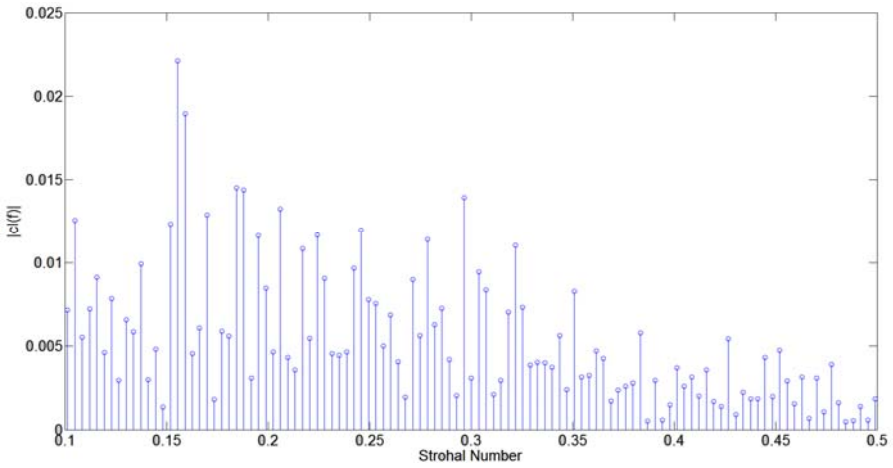

Figure 4-8 Discrete Fourier transformation result of lift oscillation of analysis around the bridge section for velocity 5.5 m/s

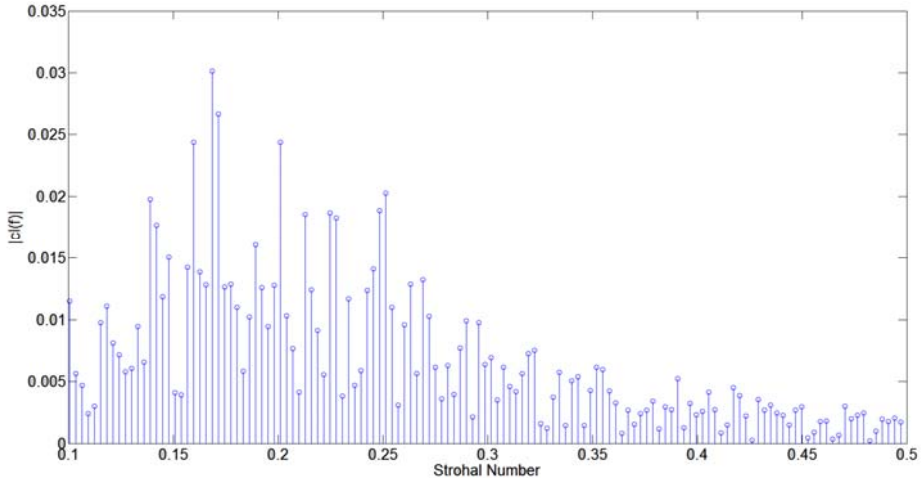

Figure 4-9 Discrete Fourier transformation result of lift oscillation of analysis around the bridge section for velocity 9.5 m/s

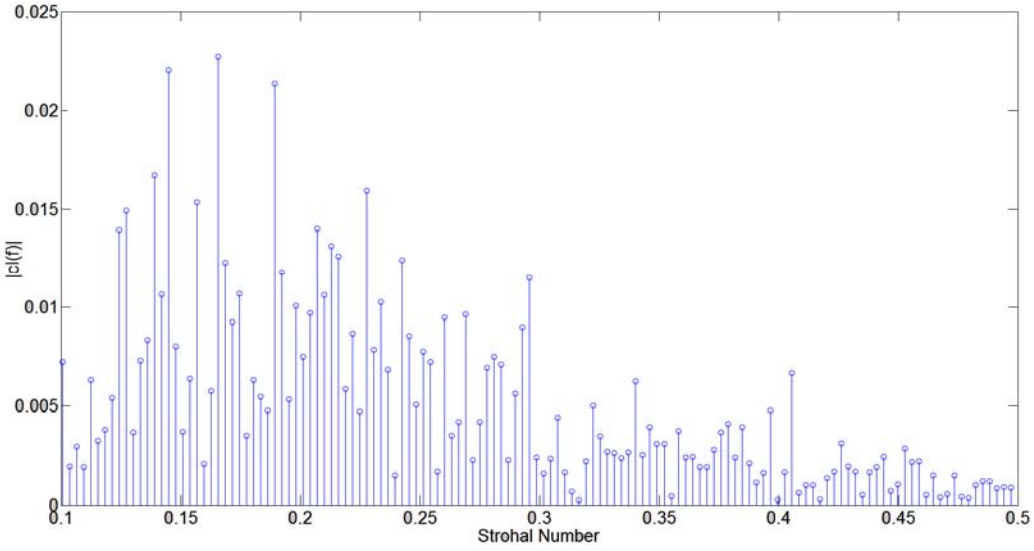

Figure 4-10 Discrete Fourier transformation result of lift oscillation of analysis around the bridge section for velocity 14 m/s

The comparison of the results is tabulated at following table (Table 4-4):

Table 4-4The comparison of the results of Strouhal numbers of the present simulation with experimental and numerical results

Velocity (m/s)	Experimental	URANS*	RVM
5.5	0.152	0.138	0.157
9.5	0.148	0.145	0.165
14.0	0.146	0.136	0.161

*URANS values are gotten by interpolation

The results given in the table for present simulation includes only the dominant frequency. But there are frequencies that have amplitudes close to the amplitude of the dominant frequency, especially for 14 m/s. Nevertheless, this is an expected phenomenon for re-attachment type bridge section, where unsteady re-attachments occurs, and is strong interaction between vortices shed from upstream and downstream corners.

When the comparison table (Table 4-4) is evaluated, the results obtained from the numerical implementation are in fairly good agreement with experimental and numerical results.

4.6 Test Case: Flow Past Oscillating Bridge Cross Section

Finally, the numerical implementation is performed to solve flow past an oscillating bridge cross section, which undergoes a forced sinusoidal oscillation with the non-dimensional frequency 0.1 and amplitude of 0.1 length of the cross section in the cross flow direction at the uniform velocity of 5.5 m/s. As a cross

section, the bridge cross section around which stationary flow is solved before (Figure 4-1) is selected again.

For this simulation, flow patterns and physical quantities are considered. Flow patterns at different non dimensional times are illustrated below (Figure 4-11):

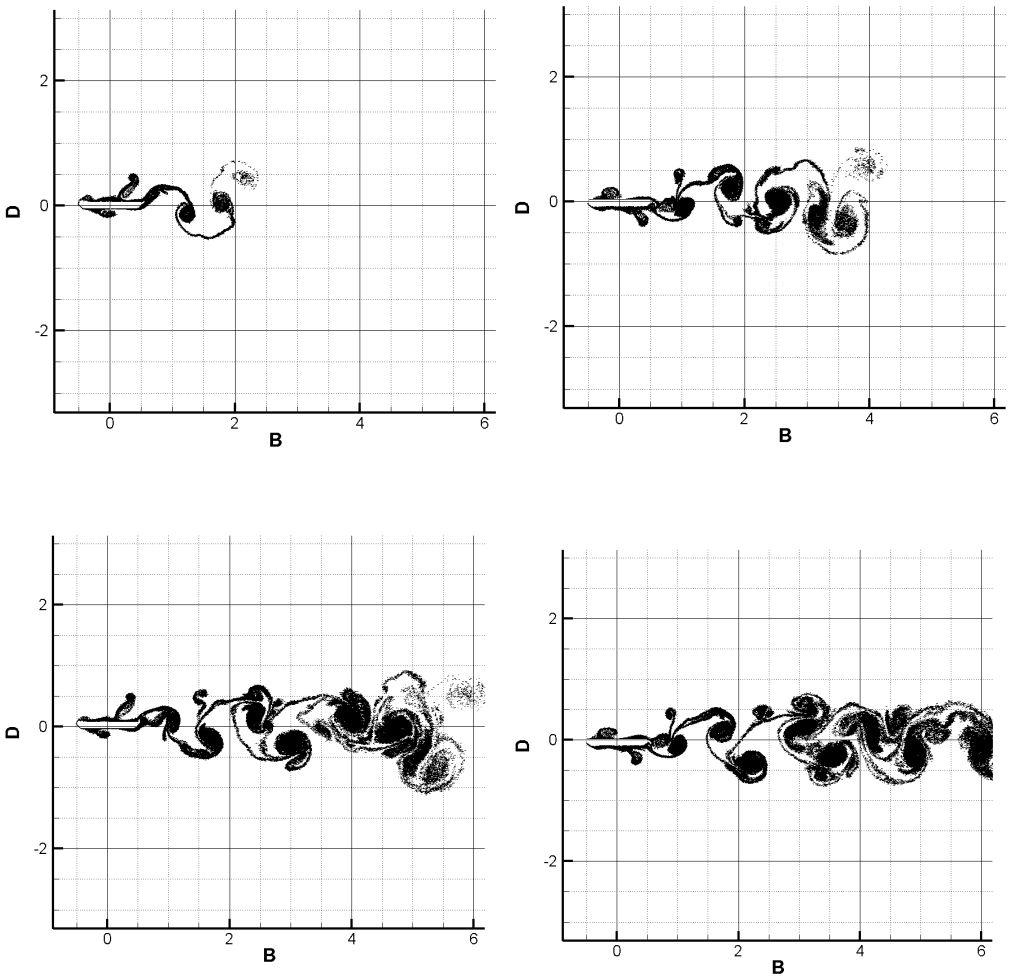

Figure 4-11 Flow around an oscillating bridge cross section at non-dimensional time (tU/B) 2, 4, 6, 8

When the flow patterns are considered, it could be seen that there is more regular vortex formation than the vortex formation obtained for flow around a stationary

bridge cross section. Because now there is only one dominant vortex shedding frequency that is the oscillation frequency of the bridge cross section. As a consequence of this event, vortices form only with this frequency, so they show more regular patterns. It could be also observed from time history of lift coefficient (Figure 4-12).

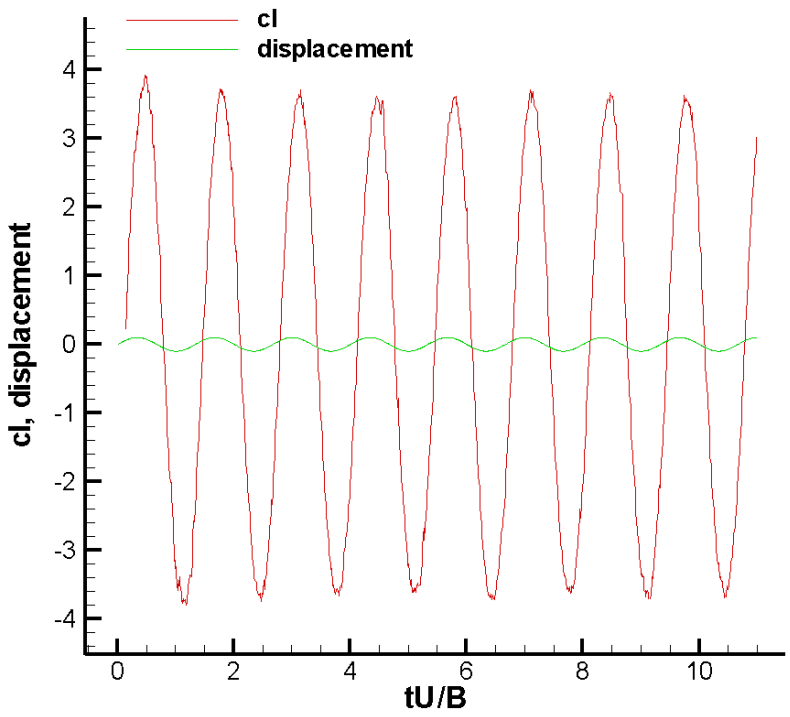

Figure 4-12 Time history of lift coefficient and bridge section displacement for flow past an oscillating bridge cross section; oscillation frequency fB/U=0.1; Y/B=0.1

CHAPTER 5

SUMMARY &CONCLUSIONS

5.1 Summary

In the present study, a random vortex method based parallel solver to analyze wind engineering problems has been developed. Its validation has been conducted by analyzing flow past bluff bodies, such as a square and a circular cylinder, a NACA 0012 airfoil at angle of attack 20^0. Moreover, having shown the applicability of the method to stationary problems, as a non-stationary problem, flow past an oscillating circular cylinder is considered.

A fairly good agreement is achieved in physical quantities with experimental and numerical results in literature for both stationary and non-stationary flow problems. Furthermore, the computer code is found generally successful to capture general flow features and patterns.

Having shown the validity and the applicability of the random vortex method based numerical implementation to bluff body problems, its application to the general wind engineering problem, flow past long-span bridge cross section, is conducted. The numerical implementation is again considered successful to solve this complex flow, when the results are compared with the numerical and experimental results of Uzol & Kurç [82]. Finally, as a test case, the numerical implementation is performed to solve the flow around an oscillating long span

bridge cross section. As a result, reasonable flow features and physical quantities are obtained.

5.2 Conclusions

As a consequence, the remarkable conclusions that can be drawn from the current study are as follows:

- The results of present work proves the random vortex method is well-suited to bluff body aerodynamics problems, in which there is a circulation region introduced by flow separation at downstream and a oscillating wake composed of vortices.
- Moreover, the results also illustrate that, the random vortex method has the potential to be a strong tool for the analysis of wind engineering problems, such as flow past long span bridge cross sections.
- Furthermore, it is found that with comparatively little effort, the random vortex method is able to analyze moving bodies, since there is no need body-fitted mesh.
- In addition to these, even the parallel implementation used in this study couldn't manage to be successful enough; it was shown that random vortex methods are suitable for parallelization.

5.3 Scope for Further Work

In order to have a more useful tool to analyze wind engineering problems, as a future work the items listed below could be implemented:

- Fast algorithms could be used for example the velocity calculation could be done by solving poisson equation with fast fourier transform instead of direct method.
- Diffusion equation could be solved by using a deterministic method such as particle strength exchange method [88].
- Parallelization could be improved, by using better algorithms and by parallelizing all subroutines in the computer code.
- Moreover, the computer code could be adapted to be run on GPU "which offers an order-of-magnitude better price performance ratios than CPUs (under 1 USD per GFlop/s for the NVIDIA 8800 GTS compared with 10-15USD for entry-level quad-core CPUs) with increasingly less restrictive programmability" [89].
- Finally, the code could be improved to be able to simulate 3D unsteady viscous flows.

REFERENCES

[1] M. L. Ould-Salihi, G.-H. Cottet, M. E. Hamraoui, “Blending finite-difference and vortex methods for incompressible flow computations”, SIAM J. Sci. Comput. 22 (5), 1655-1674, 2000.

[2] Strouhal, V., "Uber eine besondre Art der Tonerregung". Ann. Phys. und Chemie. Nav. Series 5, 216-51, 1878.

[3] Karman, Th. von, "Uber den Mechanismus des Widerstandes, den ein bewegter Korper in einer Flussigkeiterfahrt". Gottingen Nachrichten Maths.-Phys. KI., 509-17., 1911.

[4] Rosenhead, L., "The formation of vortices from a surface of discontinuity". Proc. Roy. Soc. A., 134, 170-92, 1931.

[5] Birkhoff, G. & Fisher, J., "Do vortex sheet roll up?". Rendi. Circ. Mat. Palermo, Ser. 2, 8, 77-80, 1959.

[6] Abernathy, F. H. & Kronauer, R. E., "The formation of vortex streets"., J. Fluid Mech., 13, 1-20, 1962.

[7] A. J. Chorin, P. S. Bernard, "Discretization of a vortex sheet, with an example of roll-up", J. Comput. Phys. 13 (3) 423-429, 1973.

[8] K. Kuwahara, H. Takami, "Numerical studies of two-dimensional vortex motion by a system of point vortices", J. Physical Society of Japan 34 (1) 247-253, 1973.

[9] O. H. Hald, "The convergence of vortex methods", II, SIAMP J. Numer. Anal. 16 (5) 726-755, 1979.

[10] O. H. Hald, V. D. Prete, "Convergence of vortex methods for Euler's equations", Math. Comput. 32 791-809, 1978.

[11] J. T. Beale, A. Majda, "Vortex methods II: Higher order accuracy in two and three dimensions", Math. Comput. 29 (159), 29-52, 1982.

[12] A. J. Chorin, "Numerical study of slightly viscous flow", J. Fluid Mech. 57 785-796, 1973.

[13] Roberts, S. G., "Accuracy of the random vortex methods for a problem with non-smooth initial conditions". Journal of Computational Physics, 58, 29-43, 1985.

[14] Chorin, A. J. "Vortex models and boundary layer instability". SIAM J. Sci. Stat. Comput. 1, 1, 1–21, 1980.

[15] Porthouse, D. T. C. & Lewis, R. I., "Simulation of viscous diffusion for extension of the surface vorticity method to boundary and separated flows". J. Mech. Eng. Sci., I. Mech. E., 23, No. 3, 157-67, 1981.

[16] A. J. Chorin, "Computational Fluid Mechanics", Academic Press, New York, 1989

[17] A. J. Chorin, "Vortex sheet approximation of boundary layers", J. Comput. Phys. 27, 428-442, 1978.

[18] M. F. McCracken and C. S. Peskin, "A vortex method for blood flow through heart valves", J. Comput. Phys. 35, 183-205, 1980.

[19] Ghoniem, A. F., and Sherman, F. S., "Grid-free simulation of diffusion using random walk methods". J. Comp. Phys. 61, 1–37, 1985.

[20] A. Y. Cheer, “Unsteady separated wake behind an impulsively started cylinder in slightly viscous fluid”, J. Fluid Mech. 201, 485-505, 1989.

[21] A. Y. Cheer, “Numerical study of incompressible slightly viscous flow past blunt bodies and airfoils”, SIAM J. Sci. Stat. Comput. 4, 685-705, 1983.

[22] Sethian, J., “Turbulent combustion in open and closed vessels”. Journal of Computational Physics, 54, 425-456, 1984.

[23] I. Mortazavi, P. Micheau, A. Giovannini, “Numerical convergence of the random vortex method for complex flows”, ESAIM Proc. 1, 521-538, 1996.

[24] Y. Gagnon, A. Giovannini, P. Hébrard, “Numerical simulation and physical analysis of high Reynolds number recirculating flows behind sudden expansions”, Phys. Fluids A 5 (10), 2377-2389, 1993.

[25] Kim, T. and M. R. Flynn. “Numerical simulation of air flow around multiple objects using the discrete vortex method”. Journal of Wind Engineering and Industrial Aerodynamics, 56, 213-234, 1995.

[26] S.-C. Wang, “Control of dynamic stall”, Ph.D. thesis, Florida State University, unpublished, 1995.

[27] Lin, H., M. Vezza, and R. A. McD. Galbraith. “Discrete vortex method for simulating unsteady flow around pitching aerofoils”. AIAA Journal, 35(3), 494-499, 1997.

[28] Taylor, I. and M. Vezza. “Prediction of unsteady flow around square and rectangular cylinders using a discrete vortex method”. Journal of Wind Engineering and Industrial Aerodynamics, 82, 247-269, 1999.

[29] Ramachandran P., “Development and study of a high-resolution two-dimensional random vortex method”, Ph.D. thesis, Indian Institute of Technology, 2004.

[30] J. T. Beale, “On the accuracy of vortex methods at large times”, in: IMA Workshop on Computational Fluid Dynamics and Reacting Gas Flows, Springer-Verlag, p. 19, 1988.

[31] J. A. Strain, “2D vortex methods and singular quadrature rules”, J. Comput. Phys. 124, 131-145, 1996.

[32] J. S. Marshall, J. R. Grant, “Penetration of a blade into a vortex core: vorticity response and unsteady blade forces”, J. Fluid Mech. 306, 83-109, 1996.

[33] H.O. Nordmark, Rezoning for higher order vortex methods, J. Comput. Phys. 97, 366-397, 1991.

[34] Stock M. J., “Summary of Vortex Methods Literature (A living document rife with opinion)”, unpublished, 2007

[35] J. R. Mansfield, O. M. Knio, C. Meneveau, “Towards Lagrangian large vortex simulation”, ESAIM Proc. 1, 49-64, 1996.

[36] G.-H. Cottet, P. Koumoutsakos, M. L. Ould-Salihi, “Vortex methods with spatially varying cores”, J. Comput. Phys. 162, 164-185, 2000.

[37] G. Daeninck, P. Ploumhans, G. S. Winckelmans, “Simulation of three dimensional bluff-body flows using vortex methods: from direct numerical simulation towards large-eddy simulation modeling”, J. Turb.3 (043), 2002.

[38] P. Moeleker, A. Leonard, “Lagrangian methods for the tensor-diffusivity subgrid model”, J. Comput. Phys. 167, 1-21, 2001.

[39] P. Chatelain, A. Leonard, “Face-centred cubic lattices and particle redistribution in vortex methods”, J. Turb. 3 (046), 2002.

[40] J. D. Eldredge, “Efficient tools for the simulation of flapping wing flows”, in: 43rd Aerospace Sciences Meeting, AIAA, 2005.

[41] D. M. Summers, T. Hanson, C. B. Wilson, “A random vortex simulation of wind-flow over a building”, International Journal for Numerical Methods in Fluids, Vol. 5, Issue 10, pg. 849-871, 1985.

[42] T.D. Bui, A.K. Oppenheim, “Evaluation of wind effects on model buildings by the random vortex method”, Applied Numerical Mathematics, Vol. 3, Issues 1–2, pg195-207, 1987.

[43] G. Turkiyyah, D. Reed, J. Yang, “Fast vortex methods for predicting wind-induced pressures on buildings”, Journal of Wind Engineering and Industrial Aerodynamics, Vol. 58, Issues 1–2, pg. 51-79, 1995

[44] N. Bazeos, D.E. Beskos, “Numerical determination of time-averaged wind loads on complex structures in 2D flows”, Engineering Structures, Vol. 16, Issue 3, pg. 190-200, 1994.

[45] B. Bienkiewicz, R. F. Kutz, “Aerodynamic loading and flow past bluff bodies using discrete vortex method”, Journal of Wind Engineering and Industrial Aerodynamics, Vol. 46–47, pg. 619-628, 1993.

[46] Preidikman, S., and Mook, D. T., “On the development of a passive damping system for wind-excited oscillations of long-span bridges”. J. Wind Engng. and Industrial Aerodynamics 77&78, 443–456, 1998.

[47] A. Larsen, J. H. Walther, “Discrete vortex simulation of flow around five generic bridge deck sections”, Journal of Wind Engineering and Industrial Aerodynamics, Vol. 77–78, pg. 591-602, 1998.

[48] Taylor, I., and Vezza, M., “Calculation of the flow field around a square section undergoing forced transverse oscillations using a discrete vortex method”. J. Wind Engng. and Industrial Aerodynamics 82, 271–291, 1999.

[49] Taylor, I., and Vezza, M. “Prediction of unsteady flow around square and rectangular section cylinders using a discrete vortex method”. J. Wind Engng. and Industrial Aerodynamics 82, 247–269, 1999.

[50] G. Morgenthal, “Aerodynamic Analysis of Structures Using High-resolution Vortex Particle Methods”, Ph.D. thesis, University of Cambridge, 2002.

[51] Lewis, R. I. "Vortex Element Methods for Fluid Dynamics Analysis of Engineering Systems". Cambridge University Press, 1991.

[52] M. Bergdorf and P. Koumoutsakos. “A Lagrangian particle-wavelet method. Multiscale modeling and simulation”, 5(3):980–995, 2006.

[53] F. H. Harlow. “Particle-in-cell computing method for fluid dynamics”. 3:319–343, 1964

[54] G. H. Cottet. “A particle-grid superposition method for the Navier-Stokes equations”. 89:301–318, 1990.

[55] P. Koumoutsakos, G.-H.Cottet and D. Rossinelli, "Simulations Using Particles: Bridging Computer Graphics and CFD", SIGGRAPH 2008 course, 2008.

[56] Roberts, S. G., “Accuracy of the random vortex methods for a problem with non-smooth initial conditions”. Journal of Computational Physics, 58, 29-43, 1985.

[57] Batchelor, G.K., “An introduction to fluid dynamics”. Cambridge University Press, 1970.

[58] S. Hoerner, "Fluid Dynamic Drag", Hoerner Fluid Dynamics, 1993.

[59] Norberg, C.."Pressure forces on a circular cylinder in crossflow". In: Eckelmann, *et. al.* (Eds.), Proceedings of IUTAM Conference on Bluff Body Wake Instabilities. Springer, Berlin, 1992

[60] Moeller, M.J., Leehey, P., "Unsteady forces on a cylinder in crossflow at subcritical Reynolds numbers". In: Paidoussis, M.P., Griffin, O.M., Sevik, M. (Eds.), ASME Symposium on Flow-Induced Vibrations, vol. 1. New Orleans, ASME, New York, pp.57–71, 1984

[61] Williamson, C. H. K., " Oblique and parallel modes of vortex shedding in the wake of a circular cylinder at low Reynolds number". J. Fluid Mech., 206:579-627, 1989.

[62] Roshko, A., "Experiments on the flow past a circular cylinder at very high Reynolds number". J. Fluid Mech., 10:345-356, 1961.

[63] Schewe, G., "On the force fluctuations acting on a circular cylinder in cross-flow from subcritical up to transcritical Reynolds numbers". J. Fluid Mech., 133:265-285, 1983.

[64] S. Dong, G.E. Karniadakis, "DNS of flow past a stationary and oscillating cylinder at Re = 10 000". Journal of Fluids and Structures, 20:519–531, 2005.

[65] A.W. Marris, "A Review on Vortex Streets, Periodic Waxes, and Induced Vibration Phenomena". Jour. Basic Engr., Vol. 86, no. 2, p. 185, 1964.

[66] Jerry M. Chen, Chia-Hung Liu, “Vortex shedding and surface pressures on a square cylinder at incidence to a uniform air stream", International Journal of Heat and Fluid Flow 20, 592-597, 1999.

[67] Lyn DA, Einav S, Rodi W, Park J.H.,"A laser-Doppler velocimetry study of ensemble-averaged characteristics of the turbulent near wake of a square cylinder. J. Fluid Mech., 304:285–319, 1995.

[68] Luo SC, Yazdani MG, Chew YT, Lee TS, "Effects of incidence and after body shape on flow past bluff cylinders". J. Wind Engng. Ind. Aero, 53:375–99, 1994.

[69] Vickery B. J., "Fluctuating lift and drag on a long cylinder of square cross-section in a turbulent stream". J Fluid Mech., 25:481–94, 1966.

[70] Norberg C. "Flow around rectangular cylinders: pressure forces and wake frequencies". J Wind Engng. Ind Aero, 49:187–96, 1993.

[71] Lee B. E., "The effect of turbulence on the surface pressure field of a square prism". J Fluid Mech., 69:263–82, 1975.

[72] Tamura T., Miyagi T. "The effect of turbulence on aerodynamic forces on a square cylinder with various corner shapes". J Wind Engng. Ind. Aero, 83:135–45, 1999.

[73] Saha A. K., Muralidhar K., Biswas G. "Experimental study of flow past a square cylinder at high Reynolds numbers". Exper. Fluids; 29: 553–63, 2000.

[74] Sohankar A., Norberg C., Davidson L., "Simulation of unsteady 3Dflow around a square cylinder at moderate Reynolds number". Phys Fluids, 11(2): 288–306, 1999.

[75] Sohankar A., Davidson L, Norberg L. "Numerical simulation of unsteady flow around a square 2D cylinder". In: Bilger R. W., editor. Proc. 12th Australasian fluid mechanics conference, pg. 517–20, 1995.

[76] G. Wang and S.P. Vanka, "LES of flow over a square cylinder". Department of Mechanical and Industrial Engineering, University of Illinois at Urbana-Champaign, USA, inhttp://ercoftac.mech.surrey.ac.uk/LESig/les2/

[77] M. Porquie, M. Breuer and W. Rodi. "Computed test case: square Cylinder. Institute for hydromechanics", University of Karlsruhe, Germany, inhttp://ercoftac.mech.surrey.ac.uk/LESig/les2

[78] D. Lyn and W. Rodi, "The flaping shear layer formed by flow separation from the forward corner of a square cylinder". J. Fluid Mech., 267, pp. 353-376, 1994.

[79] D. Lyn, S. Einav W. Rodi and J. Park, "A laser doppler velocimetry study of ensemble-averaged characteristics of the turbulent near wake of a square cylinder". J. Fluid Mech.,304, pp. 285-319, 1995.

[80] Sheldahl, R. E. and Klimas, P. C., "Aerodynamic characteristics of seven airfoil sections through 180 degrees angle of attack for use in aerodynamic analysis of vertical axis wind turbines", SAND80-2114, Sandia National Laboratories, Albuquerque, New Mexico, March 1981.

[81] Gopalkrishnan, R.,."Vortex-induced forces on oscillating bluff cylinders". Ph.D. Thesis, Department of Ocean Engineering, MIT, Cambridge, MA, USA, 1993

[82] Uzol O., Kurç Ö.,. "Uzun açıklıklı köprü kesitlerinin rüzgar altındaki davranışının analitik ve deneysel incelemesi", Tübitak project no: 110M799, 2012.

[83] H. Nakaguchi, K. Hashimoto and S. Muto, "An experimental study on aerodynamic drag of rectangular cylinders", J. Japan Sot. of Aeronautical and Space Sci. 16 (168), 1-5, 1968.

[84] K. Shimada and T. Ishihara, "Prediction of aeroelastic vibrations of rectangular cylinder by k-ε model", J. Aerospace Eng. 4 (12), 122-135, 1999.

[85] A. Okajima, "Flow around a rectangular cylinder with a series of various width/height ratios", J. Wind Eng.17, 1-19, 1983.

[86] N. Shiraishi and M. Matsumoto, "On classification of vortex-induced oscillation and its application for bridge structures". J. Wind Eng. Ind. Aerodyn. 14, 419-430, 1983.

[87] L. Bruno, S. Kris, "The Validity of 2D Numerical Simulations of Vertical Structures Around a Bridge Deck", Mathematical and Computer Modelling 37, 795-828, 2003.

[88] S. Mas-Gallic, Contribution al analyse numerique des methodes particulaires, Ph.D. thesis, Universite Paris VI, 1987.

[89] Stock, M. J. and Gharakhani, A., “Toward Efficient GPU-accelerated N-body Simulations,” 46th AIAA Aerospace Sciences Meeting and Exhibit, Reno, Nevada, pp. 608–621, January 7–10, 2008.